Genomics of perivascular space burden unravels early mechanisms of cerebral small vessel disease

Stéphanie Debette (stephanie.debette@u-bordeaux.fr)
University of Bordeaux, Inserm, Bordeaux Population Health Research Center, team VINTAGE, UMR 1219; Department of Neurology, Bordeaux University Hospital, Institute for Neurodegenerative Diseases

Marie-Gabrielle Duperron
University of Bordeaux, Inserm, Bordeaux Population Health Research Center, team VINTAGE, UMR 1219

Maria Knol
Erasmus MC University Medical Center https://orcid.org/0000-0002-3597-1531

Quentin Le Grand
University of Bordeaux, Inserm, Bordeaux Population Health Research Center, team VINTAGE, UMR 1219
https://orcid.org/0000-0002-9299-0747

Tavia Evans
Department of Clinical Genetics, and Department of Radiology, Erasmus Medical Centre, Rotterdam

Aniket Mishra
University of Bordeaux, Inserm, Bordeaux Population Health Research Center, team VINTAGE, UMR 1219

Gennady Roshchupkin
Erasmus MC Medical Center https://orcid.org/0000-0002-3403-2313

Takahiro Konuma
Department of Statistical Genetics, Osaka University Graduate School of Medicine and Central Pharmaceutical Research Institute, JAPAN TOBACCO INC, 569-1125, Takatsuki

David-Alexandre Trégouët
INSERM, UMR_S937, ICAN Institute, Université Pierre et Marie Curie

Jose Romero
Neurology Department, Boston University School of Medicine and The Framingham Heart Study, Framingham, MA
https://orcid.org/0000-0002-1101-2950

Stefan Frenzel
Department of Psychiatry and Psychotherapy, University Medicine Greifswald

Michelle Luciano
Psychology, University of Edinburgh

Edith Hofer
Medical University Graz

Mathieu Bourgey
McGill University Genome Centre https://orcid.org/0000-0002-8432-834X

Nicole Dueker
John P. Hussman Institute for Human Genomics, University of Miami

Pilar Delgado

Institut de Recerca Vall d'hebron. Neurovascular Research Lab. Hospital Universitari Vall d'Hebron. Neurology Department. Universitat Autònoma de Barcelona. Barcelona

Saima Hilal

National University of Singapore

Rick Tankard

Centre for Healthy Brain Ageing, UNSW, Sydney, NSW 2052, Australia https://orcid.org/0000-0002-8847-9401

Florian Dubost

Department of Medical Informatics, Erasmus MC University Medical Center, Rotterdam, the Netherlands

Jean Shin

Hospital for Sick Children/University of Toronto https://orcid.org/0000-0001-7353-5178

Yasaman Saba

University of Bordeaux, Inserm, Bordeaux Population Health Research Center, team VINTAGE, UMR 1219, F-33000 Bordeaux, France

Nicola Armstrong

Department of Mathematics and Statistics, Curtin University, Perth, WA 6102, Australia

Constance Bordes

University of Bordeaux, Inserm, Bordeaux Population Health Research Center, team VINTAGE, UMR 1219, F-33000 Bordeaux, France

Mark Bastin

Centre for Clinical Brain Sciences, University of Edinburgh

Alexa Beiser

Department of Biostatistics, Boston University School of Public Health

Henry Brodaty

Centre for Healthy Brain Ageing https://orcid.org/0000-0001-9487-6617

Robin Bülow

Institute for Diagnostic Radiology and Neuroradiology, University Medicine Greifswald, Greifswald https://orcid.org/0000-0003-1884-5784

Caty Carrera

Stroke Pharmacogenomics and Genetics. IIB-Sant Pau. Barcelona, Spain.

Christopher P. Chen

National Cancer Center

Ching-Yu Cheng

Singapore Eye Research Institute, Singapore National Eye Centre; Ophthalmology and Visual Sciences Academic Clinical Program (Eye ACP), Duke-NUS Medical School, Singapore https://orcid.org/0000-0003-0655-885X

Ian Deary

University of Edinburgh

Piyush G. Gampawar

Gottfried Schatz Research Center (for Cell Signaling, Metabolism and Aging), Medical University of Graz, Austria

Jayandra Himali

Glenn Biggs Institute for Alzheimer's and Neurodegenerative Diseases and Department of Population Health Sciences, UT Health San Antonio, San Antonio, TX, USA

Jiyang Jiang

Centre for Healthy Brain Ageing, UNSW, Sydney, NSW 2052, Australia

Shuo Li
Boston University https://orcid.org/0000-0003-2331-2448
Melissa Macalli
University of Bordeaux, Inserm, Bordeaux Population Health Research Center, team HEALTHY, UMR 1219, F-33000 Bordeaux, France
Pascale Marquis
Department of Human Genetics, McGill University, Montreal, QC Canada
Zoe Morris
Neuroradiology Department, Department Of Clinical Neurosciences, Western General Hospital, Edinburgh, UK
Susanna Muñoz Maniega
Brain Research Imaging Centre, University of Edinburgh, Edinburgh, EH4 2XU, UK.
Matthew Paradise
Centre for Healthy Brain Ageing, UNSW, Sydney, NSW 2052, Australia
Parva Pedram
Radiology Department, Boston University School of Medicine
Tatjana Rundek
Department of Neurology and Evelyn F. McKnight Brain Institute, Miller School of Medicine, University of Miami, Miami, FL, USA
Murali Sargurupremraj
University of Bordeaux, Inserm, Bordeaux Population Health Research Center, team VINTAGE, UMR 1219, F-33000 Bordeaux, France; Glenn Biggs Institute for Alzheimer's & Neurodegenerative Diseases Unive
Sabrina Schilling
University of Bordeaux, Inserm, Bordeaux Population Health Research Center, team VINTAGE, UMR 1219, F-33000 Bordeaux, France
Omar (TBC) Soukarieh
University of Bordeaux, Inserm, Bordeaux Population Health Research Center, team VINTAGE, UMR 1219, F-33000 Bordeaux, France
Alexander Teumer
University Medicine Greifswald https://orcid.org/0000-0002-8309-094X
Anbupalam Thalamuthu
University of New South Wales, Australia
Julian Trollor
Centre for Healthy Brain Ageing, UNSW, Sydney, NSW 2052, Australia
Ami Tsuchida
University of Bordeaux, Institue for Neurodegenerative Disorders, UMR5293, F-33076 Bordeaux, France
Maria Valdés Hernández
Centre for Clinical Brain Sciences, University of Edinburgh & Brain Research Imaging Centre, University of Edinburgh
Meike Vernooij
Erasmus University Medical Center
Uwe Völker
Greifswald University Hospital
Katharina Wittfeld

German Center for Neurodegenerative Diseases (DZNE), Site Rostock/ Greifswald https://orcid.org/0000-0003-4383-5043

Tien Yin Wong

Singapore Eye Research Institute, Singapore

Margaret Wright

Queensland Brain Institute, The University of Queensland, Brisbane 4072, Australia

Qiong Yang

Boston University School of Public Health

Junyi Zhang

Peking University Medical College Hospital, Beijing 107730, China

Wanting Zhao

Singapore Eye Research Institute, Singapore

Ycheng Zhu

Peking University Medical College Hospital, Beijing 107730, China

Helena Schmidt

Gottfried Schatz Research Center (for Cell Signaling, Metabolism and Aging), Medical University of Graz, Austria

Perminder Sachdev

University of New South Wales https://orcid.org/0000-0002-9595-3220

Wei Wen

University of New South Wales https://orcid.org/0000-0003-2753-3870

Anne JOUTEL

Institute of Psychiatry and Neuroscience of Paris, INSERM U1266, Université Paris Descartes, Paris

Claudia Satizabal

Glenn Biggs Institute for Alzheimer's and Neurodegenerative Diseases and Department of Population Health Sciences, UT Health San Antonio, San Antonio, TX

Ralph Sacco

Department of Neurology and Evelyn F. McKnight Brain Institute, Miller School of Medicine, University of Miami, Miami, FL, USA

Guillaume Bourque

McGill University https://orcid.org/0000-0002-3933-9656

Mark Lathrop

Department of Human Genetics, McGill University-Génome Québec Innovation Centre, Québec

Tomas Paus

University of Montreal https://orcid.org/0000-0003-1495-9338

Israel Fernandez-Cadenas

Stroke Pharmacogenomics and Genetics group, Biomedical Research Institute Sant Pau (IIB Sant Pau), Barcelona

Bernard Mazoyer

University of Bordeaux https://orcid.org/0000-0003-0970-2837

Yukinori Okada

Osaka University https://orcid.org/0000-0002-0311-8472

Hans Grabe

University of Greifswald https://orcid.org/0000-0003-3684-4208

Karen Mather

University of New South Wales, Australia

Reinhold Schmidt

Medical University of Graz

M. Arfan Ikram

Erasmus University Medical Center https://orcid.org/0000-0003-0372-8585

Christophe Tzourio

University of Bordeaux, Inserm, Bordeaux Population Health Research Center, team HEALTHY, UMR 1219, F-33000 Bordeaux

Joanna Wardlaw

University of Edinburgh https://orcid.org/0000-0002-9812-6642

Sudha Seshadri

Boston University School of Medicine

Hieab Adams

Erasmus University Medical Center https://orcid.org/0000-0003-3687-2508

Article

Keywords:

Posted Date: October 21st, 2021

DOI: https://doi.org/10.21203/rs.3.rs-963149/v1

Version of Record: A version of this preprint was published at Nature Medicine on April 17th, 2023. See the published version at https://doi.org/10.1038/s41591-023-02268-w.

Abstract

Perivascular space burden (PVS) is an emerging and possibly the earliest magnetic resonance imaging (MRI)-marker of cerebral small vessel disease (cSVD), a leading cause of stroke and dementia. Its molecular underpinnings are unknown. Genome-wide and whole-exome association studies in 40,095 participants (21 population-based cohorts, 66.3±8.6 years) revealed 24 genome-wide significant PVS risk loci. These showed association with white matter PVS already at age 20, suggesting an important role of early-life factors. PVS loci were enriched in genes causing early-onset leukodystrophies and genes expressed in fetal brain endothelial cells. Mendelian randomization analyses supported causal associations of high blood pressure with basal ganglia (BG) and hippocampal PVS, and of BG PVS with stroke. Transcriptome-wide association studies suggest causal implication of 11 genes, to prioritize for experimental follow-up as putative biotargets for cSVD. Two-thirds of PVS loci point to novel pathways, involving extracellular matrix, membrane transport, and developmental processes, with enrichment in targets of existing drugs for vascular/cognitive disorders.

Introduction

Perivascular spaces (PVS), also named Virchow-Robin spaces, are physiological spaces surrounding small vessel walls as they run from the subarachnoid space through the brain parenchyma.[1,2] Dilation of PVS, as observed on brain magnetic resonance imaging (MRI), is thought to be a marker of perivascular space dysfunction and, by implication from preclinical studies, is speculated to reflect impairment of brain fluid and waste clearance.[3–5]

PVS increase in number with age and vascular risk factors, especially hypertension.[6,7] They are associated with white-matter hyperintensities (WMH) of presumed vascular origin, lacunes, and cerebral microbleeds (CMB),[4,8,9] all MRI features of cerebral small vessel disease (cSVD), a leading cause of stroke and dementia with no specific mechanistic treatments to date.[10,11] PVS can be detected on brain MRI much earlier than WMH, lacunes, or CMB,[4] and are also described as the earliest stage of cSVD lesions on neuropathology.[12] Their pathophysiology is poorly understood.[11,13]

In experimental models, PVS appear to be important conduits for substrate delivery, flushing interstitial fluid, clearing metabolic waste (such as beta amyloid peptide, the accumulation of which is a hallmark of Alzheimer disease [AD]), and brain fluid regulation, as part of the “glymphatic system”.[4,5] These processes were described to increase during sleep.[3–5, 14] Whether perivascular spaces have similar functions in humans is unclear. Several studies have suggested an association of PVS burden (number of visible PVS on brain MRI) with stroke,[3,11,15–18] AD pathology, and cerebral amyloid angiopathy.[19,20] Post-stroke edema has been linked to post-stroke enlargement of perivascular spaces,[21] and PVS dilation was observed in amyotrophic lateral sclerosis patients with perivascular fibroblast proteins being associated with survival. Thus there is mounting evidence for a major role of PVS in cerebral injury.[22]

High heritability of PVS burden suggests an important contribution of common genetic variants,[23] the identification of which could be a powerful tool to decipher underlying biological pathways. We conducted genome-wide association study (GWAS) meta-analyses and whole exome/genome sequencing studies of extensive PVS burden in 40,095 and 19,010 participants respectively. Given previously reported differential risk factor profiles,[3,7,24] we ran analyses separately for PVS in the white matter (WM), basal ganglia (BG) and hippocampus (HIP). We explored associations of identified risk loci on PVS burden in young healthy adults and examined shared genetic

determinants with other MRI-markers of brain aging, putative risk factors, and common neurological diseases. We conducted extensive bioinformatics exploration of identified PVS risk loci, leveraging complementary large-scale biological resources ranging from tissue and cell-specific gene expression databases to drug target libraries.

Results

Genetic discovery

A total of 21 population-based cohorts were included in the analyses, of which 18 for GWAS and 8 (5 of which also contributed to the GWAS) for whole exome association studies (**Supplementary Table 1**). We tested associations of extensive PVS burden with ~8 million common and low-frequency (minor allele frequency [MAF] 1-5%) single nucleotide polymorphisms (SNPs) in GWAS meta-analyses of 40,095 older participants from 18 population-based cohorts (mean age 66.3±8.6 years, 51.7% women, 66.7% hypertensives, **Supplementary Table 1-3**). Of these 9,642, 9,165, and 9,316 had extensive PVS burden in WM, BG, and HIP respectively, defined as PVS grades or numbers equal to or larger than the 75th percentile of the distribution. We dichotomized PVS burden measures because different rating scales were used across studies (**Supplementary Methods**). Participants were predominantly of European ancestry (N=38,871, 96.9%), with small minorities of Hispanics (N=717), East-Asians (N=339), and African-Americans (N=168).

Stage 1 meta-analyses comprised 11,511 participants from 17 cohorts participating in the CHARGE consortium,[25] for whom WM, BG, and HIP PVS (Figure 1) were rated primarily on visual semi-quantitative rating scales.[7,26–29] Using ancestry-specific sample-size weighted meta-analyses followed by meta-analyses across ancestries, we identified 2 genome-wide significant risk loci ($p<5x10^{-8}$) for WM PVS at chr9q31.3 (intron of *LPAR*1) and chr3p25.1 (near *LINC00620*/ *WNT7*, Table 1, Figure 1). The lead variants of both of these loci replicated in 28,500 UK Biobank (UKB) participants using a novel computational method to quantify PVS[30] ($p<1.15x10^{-8}$, **Supplementary Table 5**). A third locus at chr20q13.12 (intron of *SLC13A3*) reaching near genome-wide significance in stage 1 ($p=8.67x10^{-8}$) also replicated in UKB ($p=3.36x10^{-20}$).

In stage 2 we meta-analyzed stage 1 and UKB association statistics. We identified 22 independent genome-wide significant risk loci for extensive PVS burden (WM PVS: 19, BG PVS: 2, HIP PVS: 3 of which 2 were shared with WM PVS, Table 1, Figure 1, **Methods, Supplementary Figures 1-2**). Two additional loci showed genome-wide significant associations with WM PVS in Europeans only, leading to 24 independent signals (Table 1, **Supplementary Figures 1-2**). There was no systematic inflation of association statistics (**Supplementary Table 4** and **Supplementary Figure 1**).

We performed conditional logistic regression using GCTA-COJO[31] to verify whether some genome-wide significant loci harbored independent association signals. Consistent with the LD-clumping, the GCTA-COJO analysis suggested 2 independent signals at chr3p25.1 (*WNT7A*) and 6 at chr20q13.12 (*SLC13A3*, **Supplementary Figure 2, Supplementary Table 6**), four of which with low frequency or rare variants (Table 1). Haplotype analyses in the European-ancestry 3C-Dijon cohort (N=1,500) (**Supplementary Results**) suggest that 3 SNPs (rs112407396, rs2425881 and rs2425884) are enough to characterize the pattern of association between the chr20q13.12 locus and WM PVS. The two common rs2425881-A and rs2425884-C alleles, in very low LD with each other (r^2~0.05, D'~0.50), generated a common (frequency ~0.50) haplotype associated with WM PVS (OR=1.25[95%CI:1.05-1.49]). The effect of this haplotype was amplified by 1.7 in the presence of the rs112407396-T allele (MAF=0.02), which

has a high probability to be a regulatory variant (HaploReg, GTex, RegulomeDB, **Supplementary Results**). Using MR-MEGA there were no loci showing high heterogeneity in allelic effects across ancestries (PHet<0.01) and reaching genome-wide significance (**Supplementary Table 7**).

Gene-based association analyses in European-ancestry participants using MAGMA[32] identified 28 gene-wide significant associations at $p<2.63x10^{-6}$. Of these, 12 were in 8 loci not reaching genome-wide significance in the GWAS meta-analyses (WM PVS: 3 [*INS-IGF2/IGF2, PRKAG2*, and *LRP4/CKAP5*], BG PVS: 4 [*SH3PXD2A, WNT3, ZMYND15*, and *KCNRG/TRIM13/SPRYD7*], and HIP PVS: 1 [*PDZRN4*], Figure 1, **Supplementary Table 8**). Using VEGAS,[33] we identified one additional gene (*NSF*) for BG PVS in the same locus as *WNT3* (**Supplementary Table 8**). All were in suggestive GWAS loci ($p<5x10^{-6}$, **Supplementary Table 9**).

Using LD-score regression we estimated heritability at 11% for WM PVS, 5% for BG PVS, and 8% for HIP PVS (**Supplementary Table 10**). We found a moderate genetic correlation between BG PVS and HIP PVS (r_g(SD)=0.63(0.14); p-value=$7.23x10^{-6}$), while the genetic correlation between WM and BG or HIP PVS was modest (r_g <0.30, **Supplementary Table 10**). The genetic correlation between PVS in CHARGE (stage 1) and UKB was moderate to high for WM and HIP PVS and weaker for BG PVS (**Supplementary Table 11**).

To increase statistical power we conducted secondary multivariate association analyses using MTAG,[34] including summary statistics from GWAS of other cSVD markers, namely WMH volume[10] and lacunes (**Supplementary Table 12**).[35] Compared with univariate GWAS results we observed the highest gain in power for BG PVS, with 10 additional loci reaching genome-wide significance, of which two were also found for HIP PVS (*OBFC1, EVL/DEGS2*), and two were not previously genome-wide significant for any MRI-marker of cSVD (*CACNB2*, *NSF/WNT3*). One MTAG WM PVS locus (*VWA2*) was not described before with any MRI-marker of cSVD. Six loci showed greater significance in MTAG analysis than with PVS, WMH volumes or lacunes alone: at *VWA2* (WM PVS), *SH3PXD2A/STN1, COL4A2, CACNB2, NSF/WNT3* (BG PVS) and *DEGS2/EVL* (BG and HIP PVS).

Using whole exome sequencing (WES) and exome content of whole genome sequencing (WGS) data in respectively 19,010 participants from UKB (N=16,995) and the BRIDGET consortium (N=2,015) (**Supplementary Methods, Supplementary Table 1**), of whom 4,531, 4,424, and 4,497 had extensive PVS in WM, BG, and HIP respectively, we performed a whole exome association study (WEAS) to identify (rare) exonic variants associated with extensive PVS. As a significance threshold for single variant association studies we used $p<5\times10^{-8}$ for non-coding variants, and $p<4.3\times10^{-7}$ for coding variants, while for gene-based burden analyses of rare variants we used $p<2.7\times10^{-6}$, correcting for 18,449 protein coding Ensemble genes.[36] The single variant analysis identified 19 variants in the chr1q25.3 locus associated with HIP PVS, including two missense variants (rs20563 and rs20558, predicted to be benign by polyphen-2) and one splice donor insertion (rs34133998) in *LAMC1*, all in strong LD with the sentinel variant identified in the GWAS (**Supplementary Table 13**). Gene-based burden tests exploring protein modifying rare variants (MAF<0.01) did not identify any gene-wide significant association. The top associations for WM, BG, and HIP were *TAC3* (Beta(SE)=0.64(0.16), $p=9.37x10^{-5}$), *KL* (Beta(SE)=0.45(0.10), $p=6.06x10^{-6}$), and *ZNF335* (Beta(SE)=0.27(0.07), $p=7.98x10^{-5}$, **Supplementary Table 14**).

Implication across the lifespan and clinical correlates of identified PVS loci

To examine the impact of PVS risk variants across the lifecourse, we explored the association of the aforementioned PVS risk loci identified in older adults (mean age 66.3±8.6 years) with PVS burden in 1,748 young healthy adults participating in the i-Share cohort (mean age 22.1±2.3 years).[10,37] A WM PVS weighted genetic risk score (wGRS) derived from the PVS GWAS was significantly associated with WM PVS in young adults (OR=1.11 [95%CI:1.06-1.16], $p=2.62x10^{-6}$, Table 2). Individually, one WM PVS risk locus was associated with WM PVS in young adults after multiple testing correction (at *OPA1*) and two others at nominal significance (at *EFEMP1* and *SLC13A3*, Table 2). The association with WM PVS was in the same direction in young adults as in the GWAS for 17/21 (80%) risk loci (**Supplementary Figure 3**). Meta-regression showed significant modifying effects of age on genetic associations with lead variants at *OPA1* and S*LC13A3*, and a trend for *EFEMP1*, with larger effect sizes at younger ages (**Supplementary Figure 4**).

To explore clinical correlates of PVS, we first examined whether PVS risk loci (lead and proxy variants with $r^2>0.9$) were associated with MRI-markers of brain aging (cSVD markers and subcortical volumes), putative risk factors (vascular risk factors and sleep patterns), and common late-life neurological diseases (stroke, AD, Parkinson disease), using the largest published GWAS (**Methods, Supplementary Methods**). Out of 24 genome-wide significant PVS loci, five (21%) were significantly associated with WMH volume and five (21%) with blood pressure traits (in same and opposite directions), of which 2 were shared between WMH and blood pressure (Figure 2, **Supplementary Table 15)**. One WM PVS locus (at *FOXF2-FOXQ1*) was associated with WMH, all, ischemic and small vessel stroke and one BG PVS locus (at *ICA1L-NBEAL1*) with blood pressure, LDL-cholesterol, BMI, caudate volume, WMH, small vessel stroke, and AD (**Supplementary Table 15**). Overall 16 PVS loci (67%) did not show any association with other MRI-markers of cSVD or putative risk factors, pointing to novel biological pathways. Further shared genetic associations of PVS traits with other complex phenotypes based on the GWAS catalog[38] are shown in **Supplementary Table 16**.

Second, we explored genome-wide genetic correlations of PVS burden with MRI-markers of brain aging, putative risk factors, and neurological diseases using LD-score regression.[39] We observed significant ($p<7.9x10^{-4}$) genetic correlation of BG PVS with larger WMH and larger caudate nucleus volume, and of HIP PVS with larger hippocampal volume (adjusted for total intracranial volume). BG and HIP PVS showed significant genetic correlation with higher systolic blood pressure (SBP), diastolic blood pressure (DBP), any stroke and ischemic stroke (Figure 3, **Supplementary Table 10**).

Third, we used two-sample Mendelian randomization to seek evidence for a causal association of putative risk factors with PVS burden and of PVS burden with neurological diseases, using generalised summary-data-based Mendelian randomization (GSMR),[40] and confirming significant associations with Radial-MR ($p<1.19x10^{-3}$).[41] Genetically determined high SBP and DBP were significantly associated with higher BG and HIP PVS burden, with MR-CAUSE providing further support in favor of causality, especially for the relation with BG PVS (multitrait GWAS), although Radial-MR indicated some evidence of pleiotropy even after removal of outlier variants for DBP (**Supplementary Table 17**). Genetically determined short sleep was associated with lower BG PVS burden, with no significant evidence for causality in MR-CAUSE. Genetically determined BG PVS (accounting for other MRI-markers of cSVD) was associated with an increased risk of stroke, ischemic stroke, and small vessel stroke, with significant evidence for a causal model in MR-CAUSE for all stroke and ischemic stroke (**Supplementary Table 17**).

Functional exploration of identified PVS loci

Using MAGMA and VEGAS2Pathway we identified significant enrichment of PVS loci in pathways involved in extracellular matrix (ECM) structure and function, lymphatic endothelial cell differentiation, cell motility, and thyroid hormone transport (**Supplementary Tables 18-19**).

Genes closest to PVS lead risk variants were significantly enriched in genes mutated in OMIM syndromes associated with leukodystrophy, leukoencephalopathy, or WMH (**Supplementary Table 20**), culminating in a 20-fold enrichment in genes containing an intragenic lead variant (Figure 4). The enrichment was even stronger (30-fold) when focusing on WM PVS loci only, comprising several genes involved in early onset leukodystrophies (monogenic disorders with selective and primary involvement of the brain white matter):[42] *GFAP* (chr17q21.31), mutations of which cause Alexander disease, a rare neurodegenerative disorder of astrocytes leading to psychomotor regression and death;[43] *SLC13A3* (chr20q13.12), causing acute reversible leukoencephalopathy with increased urinary alpha-ketoglutarate;[44] and *PNPT1* (chr2p16.1), causing Aicardi-Goutières syndrome and cystic leukoencephalopathy (Figure 4).[45,46]

Although several genes near PVS lead risk variants were described to be involved in glioma (*TMEM212, NBEAL1, LPAR1, WNT7A, ITGB5, EFEMP1, LAMC1, OPA1, CALD1*, and *ISYNA1*) we found no significant enrichment for glioma genes from the COSMIC catalogue.[41]

To seek evidence for a causal implication of specific genes and variants in observed associations, we performed transcriptome-wide association studies (TWAS) using TWAS-Fusion,[47] with European PVS GWAS summary statistics and the GTEX v7 multi-tissue (RNA-seq) database, focusing on brain, vascular and blood tissues. We found 36 transcriptome-wide significant expression-trait associations for WM PVS, 25 for BG PVS, and 8 for HIP PVS that were significant conditionally on the GWAS effect at that locus and in colocalization analyses (TWAS-COLOC), providing evidence of a shared causal variant between the corresponding gene expression and PVS (**Supplementary Table 21**). Most genes were in genome-wide significant PVS risk loci: 8 genes in 5 WM GWAS loci (*C6orf195, ITGB5, LPAR1, LRRC25, RP11-71H17.9, SLC20A2, SMIM19, UMPS*), 2 genes in 1 BG PVS GWAS locus (*ICA1L*, *NBEAL1*), and 1 gene in a HIP PVS GWAS locus (*LAMC1*) (Figure 5). Additionally, PVS were associated with up- or downregulation of 9 genes outside GWAS loci requiring confirmation. TWAS-COLOC signals were mostly observed in brain tissues (17 genes), but also vascular tissues (10 genes) and blood (2 genes).

To identify enrichment in specific vascular brain cell types, we used a recently developed pipeline that combines three cell-type enrichment methods, stratified LDscore,[39,48] MAGMA,[32] and MAGMA-human (**Supplementary Table 22**).[32,49] There was a significant enrichment in brain vascular endothelial cells for all three PVS locations, based on a human single cell atlas of fetal gene expression,[50] and significant enrichment in pericytes and astrocytes for WM PVS (**Supplementary Table 23**).

Using complementary datasets quantifying gene expression in the brain from development to adulthood,[51] we explored the expression pattern of genes nearest to PVS loci prioritizing TWAS-COLOC genes (**Supplementary Figure 5**). Several WM PVS genes showed constant expression levels throughout the lifecourse (e.g. *OPA1*, *LRRC25*, *C6orf195*) or decreasing expression levels in the prenatal period, followed by an increase in the late prenatal period and beyond (e.g. *ITGB5, LPAR1, EFEMP1*). Other genes displayed a continuous decrease of expression levels (e.g. *LAMC1, UMPS*) throughout the lifecourse.

Finally, we conducted an exploratory search for enrichment of PVS genes in targets of drugs validated in other indications (**Methods**).[52] Using GREP,[52,53] we found significant enrichment of BG PVS genes in targets for

antiinfectives, driven by *CRHR1* (chr17q21.31), a target for telavancin, and for diseases of the nervous system, driven by *MAPT* (chr17q21.31), a target for davunetide; of HIP PVS genes in targets of drugs for ear diseases, driven by *SERPIND1* (chr22q11.21) a target for sulodexide, also used for the prevention of venous thrombosis (**Supplementary Figure 6**). Using TRANS-PHAR,[54] we observed significant enrichment of TWAS significant HIP PVS genes in drugs for vascular disease, including simvastatin, vincamine, and macitentan, **Supplementary Figure 7**).

Discussion

In 40,095 participants from older population-based cohorts we identified 24 genome-wide significant loci for extensive PVS burden, predominantly for WM PVS, and 6 additional loci after accounting for other MRI-markers of cSVD. In aggregate, WM PVS risk loci were significantly associated with WM PVS in 1,748 young healthy adults in their twenties. While a fifth of PVS risk loci were shared with blood pressure and WMH volume, two thirds reveal novel biological pathways, involving the ECM, membrane transport, and developmental processes, with a significant enrichment in genes expressed in fetal brain vascular endothelial cells and in genes involved in early onset leukodystrophies. Using Mendelian randomization, genetically determined high systolic and diastolic blood pressure was associated with BG and HIP PVS, while short sleep was associated with less BG PVS, and more extensive BG PVS burden with increased risk of stroke (any, ischemic, and small vessel stroke), supporting causality. Using transcriptome-wide association and colocalization analyses and screening for protein modifying variants using next generation sequencing we provide evidence for causal implication of several genes warranting experimental follow-up. We further show enrichment of PVS genes in targets for approved drugs for vascular, cognitive, and infectious diseases.

This first gene-mapping study of PVS provides completely novel insight into the biology underlying this emerging MRI-marker.[3] In line with the prevailing hypothesis that PVS is at least in part a marker of cSVD, moderate to high genetic correlation was observed with other MRI-markers of cSVD (WMH, lacunes), primarily for BG and HIP PVS. Pathway analyses point to an important involvement of ECM structure and function, previously reported to play an important role in cSVD.[10,55] Several PVS risk loci (at *FOXF2*, *EFEMP1*, *KCNK2*, and *NBEAL1-ICA1L*) are previously reported risk loci for WMH and small vessel stroke, respectively features of covert and overt cSVD.[10,56,57] The multitrait GWAS accounting for WMH reveals several additional genome-wide significant risk loci for PVS, encompassing two genes harboring mutations causing monogenic forms of SVD (at *COL4A1-COL4A2*, causing Collagen 4A1 and Collagen 4A2 microangiopathy, and *STN1*, causing COATS-plus cerebroretinal microangiopathy).[58,59] Consistent with epidemiological observations of distinct risk factor profiles,[3,7,16,24] the genetic architecture of PVS differed substantially across PVS locations, with WM PVS having a low genetic correlation with BG and HIP PVS, in line with distinct anatomical characteristics (single versus double periarterial layer of leptomeninges).[1,3,60]

Strikingly, in aggregate genetic determinants of PVS discovered in older populations appeared to already show a highly significant association with WM PVS in young healthy adults in their twenties. This corroborates a recently described association of genetic risk variants for WMH with subtle changes in MRI-detected white matter microstructure at age twenty.[10] PVS have been described very early in life,[4,61] and whether extensive PVS burden at age 20 already reflects early stages of a disease or variations in brain maturation that may modulate risk of later onset disease is unclear. The significant enrichment of PVS risk loci in genes involved in early-onset leukodystrophies, and in fetal brain vascular endothelial cells,[50] support an involvement of developmental processes. Interestingly, in the spontaneously hypertensive stroke prone rat, that closely models cSVD, intrinsic

endothelial cell dysfunctions have been observed at birth, including reduced tight junctions and heat shock protein secretion that blocks oligodendrocyte maturation, affecting myelination.[62] At PVS loci showing significant (*OPA1)* or nominally significant *(SLC13A3* and *EFEMP1*) associations with WM PVS in young adults, the larger effect size of genetic associations with decreasing age further supports early life mechanisms. *OPA1* encodes a nuclear-encoded mitochondrial protein that helps regulate mitochondrial stability and energy output, with usually a stable brain expression pattern throughout the lifecourse. Mutations in *OPA1* cause autosomal dominant optical atrophy, sometimes associated with multiple-sclerosis like illness, syndromic parkinsonism and dementia.[63] These observations are in line with epidemiological associations of early life factors such as birth parameters, childhood cognitive ability, education, or socio-economic status with worse cSVD in older age.[64]

The combination of PVS GWAS findings with gene expression quantitative loci in relevant tissues (TWAS), and with next generation sequencing data (WEAS), strongly supports putative causal genes at several loci. Some genes point to brain developmental processes, blood brain barrier (BBB) function, and response to brain damage. At chr9q31.3, WM PVS associates with lower *LPAR1* expression in vascular tissues. *LPAR1* encodes a receptor for lysophosphatidic acid, an extracellular signaling small lipid[65] implicated in brain development[66] and repair after brain injury.[67] *LPAR1* is expressed in oligodendrocytes and involved in post-natal myelination.[68] Variants in *LPAR1* are associated with functional connectivity across brain regions.[69] In a model of transient arterial occlusion, an LPAR1 antagonist attenuated brain damage after reperfusion by decreasing inflammation.[70] Modulation of LPAR1 activity may also impact neural regeneration.[71] Several drugs targeting LPAR1 are available (e.g. antidepressant mirtazapine[72]) or in development.[73] Although not significant in TWAS-COLOC, which is limited to adult bulk tissues available in GTEX, *WNT7A* at chr3p25.1 is also a strong biological candidate, encoding a secreted signaling protein that targets the vascular endothelium.[74] WNT7A is produced by the neuroepithelium of the developing central nervous system and has been implicated in brain angiogenesis and BBB regulation.[74] In transgenic mouse models, loss of Wnt7a/b function blunts the angiogenic response to hypoxia, resulting in severe white matter damage.[75]

Other genes are involved in ECM structure and function. At chr3q21.2, WM PVS was associated with lower *ITGB5* expression in whole blood. *ITGB5* encodes a beta subunit of integrin, a family of transmembrane receptors that facilitate cell-cell and cell-ECM adhesion, and is involved in adhesion to vitronectin, which plays a central role in monogenic SVD.[76] Higher ITGB5 plasma levels were recently associated with decreased odds of cognitive impairment or dementia, lower brain amyloid burden and slower brain atrophy rates.[77] At chr1q25.3, HIP PVS was associated with lower *LAMC1* expression in brain tissues and higher expression in vascular tissues. WEAS also implicates *LAMC1* at this locus, with the identification of a genome-wide significant splice donor variant. *LAMC1* encodes Laminin gamma-1, the most ubiquitously expressed laminin subunit. Laminins, a family of ECM glycoproteins, are the major noncollagenous constituent of basement membranes. Genes encoding other basement membrane proteins, *NID2* and *COL4A1/2*, have previously been implicated in other cSVD phenotypes (WMH, small vessel stroke).[10,56] Laminin regulates blood vessel diameter independent of flow,[78] and laminin expressed by astrocyte endfeet plays a major role in BBB regulation, in part through pericyte differentiation.[79] Loss of astrocytic laminin decreases expression of tight junction proteins and aquaporin-4 (AQP4),[79] thought to be a key modulator of glymphatic flow in experimental models.[4] Laminin is also involved in regulating blood brain barrier integrity and function.[79,80] *LAMC1* expression in the hippocampus decreases linearly with advancing age in humans (**Supplementary Figure 4**). Several of the aforementioned genes and additional ECM genes identified in the multivariate analysis encode families of proteins described in the cerebrovascular matrisome, perturbations of

which were recently proposed as a convergent pathologic pathway in cSVD (*LAMC1, EFEMP1, COL4A2, SH3PXD2A, VWA2*).[10,55]

Some genes point to complex pleiotropic mechanisms. At chr2q33.2, BG PVS was associated with higher expression of *ICA1L* in brain tissues and of *NBEAL1* in vascular tissues. Similar patterns have been observed recently for these genes in TWAS of WMH volume and lacunar stroke,[10,56] and BG PVS risk variants at this locus are associated with high LDL-cholesterol, BMI, WMH volume, low SBP and DBP, and increased risk of AD and small vessel stroke.[10,57,81,82] *ICA1L* (encoding islet cell autoantigen 1 like) is predominantly expressed in endothelial cells and harbors mutations causing juvenile amyotrophic lateral sclerosis,[83] while *NBEAL1* (encoding neurobeachin-like 1 protein) regulates cholesterol metabolism by modulating LDL-receptor expression.[84]

Our study points to an important involvement of solute carriers (SLCs) in PVS pathophysiology. The most significant PVS risk variants involve an intronic haplotype of *SCL13A3*, encoding a plasma membrane Na+/dicarboxylate cotransporter expressed in kidney, astrocytes, and choroid plexus.[44] Mutations in *SLC13A3* cause acute reversible leukoencephalopathy with increased urinary alpha-ketoglutarate,[44] where SLC13A3 loss-of-function may affect elimination of organic anions and xenobiotics from the cerebrospinal fluid (CSF).[44] At the same locus, other genome-wide significant variants are located near *SLC2A10*, involved in regulation of glucose homeostasis. Mutations in this gene cause arterial tortuosity syndrome,[85] an inherited connective tissue disorder characterized by elongated and tortuous large and medium-sized arteries. An association between PVS burden and internal carotid artery tortuosity, as well as intracranial arterial dolichoectasia was described in SVD patients.[86,87] WM PVS was further associated with lower *SLC20A2* expression in brain tissue, involving a splicing quantitative trait locus regulating highly tissue-specific gene isoforms in the dorsolateral pre-frontal cortex (Figure 5). *SLC20A2* is involved in phosphate transport and harbors loss-of-function mutations causing idiopathic familial basal ganglia calcification, a neurodegenerative disorder with regional accumulation of inorganic phosphate in the ECM.[88] Suggestive associations with PVS ($p<5x10^{-6}$) near numerous additional SLC genes were observed (**Supplementary Table 9**). Two recently reported small vessel stroke risk loci also involve solute carrier genes (*SLC25A44* and *SLC39A13*),[56] pointing to an important role of SLCs in cSVD pathophysiology at large. Given their role in CSF secretion and transport of various substances at the blood-CSF barrier,[89] SLCs could potentially be involved in interstitial fluid accumulation adjacent to the perivascular spaces.[90] SLCs are the largest family of transporters and have recently been proposed as key, underexploited candidates for drug target development.[91,92]

Consistent with other SVD phenotypes we observed evidence for a causal association of SBP and DBP with PVS. This was found for BG and HIP PVS, but not WM PVS, in line with epidemiological studies.[7,93] Experimental work suggests that the perivascular pump becomes less efficient with increasing blood pressure, thus reducing net forward flow in the perivascular spaces. These effects were found to be larger at more distal locations, where arteries have thinner, less muscular walls and are too weak to maintain flexibility while supporting increased blood pressure.[94] Such hemodynamic and anatomic differences[1] could, perhaps, at least partly explain the stronger impact of blood pressure on BG and HIP PVS compared to WM PVS. Genetically determined short sleep was associated with lower BG PVS burden. Studies in rodents showed that CSF uptake into perivascular spaces and flushing of interstitial fluid are increased during sleep.[3] In humans, increased visibility of BG perivascular spaces was associated with reduced sleep efficiency and interrupted sleep.[95,96] As genetically determined short sleep is associated with greater sleep quality and efficiency,[97] our findings are in line with these observations.

The significant genetic correlation of BG and HIP PVS with any stroke and ischemic stroke and robust evidence for a causal association of BG PVS with any stroke, ischemic stroke, and small vessel stroke, using complementary Mendelian randomization approaches strongly supports the clinical relevance of PVS and its relation with cSVD. Although underpowered to describe similar relationships with hemorrhagic stroke, we also found nominally significant positive genetic correlation of BG and HIP PVS with deep intracerebral hemorrhage (**Supplementary Table 10**) and evidence for a causal relation of HIP and BG PVS with all and deep intracerebral hemorrhage (**Supplementary Table 17**), consistent with epidemiological findings.[16] Considering the association of HIP PVS with lower *LAMC1* expression in brain tissues, it is striking to note that conditional knock-out of laminin in astrocytes leads to deep intracerebral hemorrhage in adult mice.[98] This is reminiscent of known associations of variants in *COL4A1/A2*, encoding another basement membrane protein, with monogenic and multifactorial deep intracerebral hemorrhage.[81,99] Significant enrichment of PVS genes in targets of drugs validated or under investigation for vascular and cognitive disorders highlights the potential of PVS genetics for cSVD drug discovery.

This is the first study exploring the genetic determinants of PVS, using a comprehensive gene-mapping strategy and extensive bioinformatics follow-up. Limitations include the predominantly European samples and heterogeneity in PVS quantification methods across cohorts. To account for this we used a dichotomized variable, which may be less powerful than continuous measures. The genetic correlation pattern between PVS measurements in CHARGE cohorts and UKB (and the fact that all loci identified in stage 1 replicated in UKB) suggests that the phenotypes are comparable. Follow-up in independent samples, when these become available, will be warranted. In the future, wider use of computational PVS measurements may enable study of the genomics of total PVS volume and to account for differences in individual PVS volume, width, length, shape and other characteristics.[100]

In conclusion, in this first gene-mapping study of PVS, one of the earliest MRI-markers of cSVD, we describe 24 genome-wide significant risk loci, with 6 additional loci in secondary multivariate analyses accounting for other cSVD markers. Our findings provide completely novel insight into the biology of PVS across the adult lifespan and its contribution to cSVD pathophysiology, with potential for genetically informed prioritization of drug targets for prevention trials of cSVD, a major cause of stroke and dementia worldwide.

Methods

Study design

Analyses were performed on stroke-free participants from 21 population-based cohorts (18 population-based cohorts for the GWAS meta-analysis), taking part in the Cohorts for Heart and Aging Research in Genomic Epidemiology (CHARGE) consortium, the BRrain Imaging, cognitive, Dementia, and next-generation Genomics (BRIDGET) initiative, and from the UK Biobank (UKB). Characteristics of study participants for each cohort are provided in **Supplementary Table 1-3**. All participants gave written informed consent, and institutional review boards approved individual studies.

Perivascular space burden definition

PVS were defined as fluid filled spaces with a signal identical to that of cerebral spinal fluid (CSF) of round, ovoid, or linear shape depending on the slice direction, with usually a maximum diameter smaller than 3 mm, and located in areas supplied by perforating arteries. PVS do not have a hyperintense rim on T2-weighted or FLAIR sequences.[9]

In most CHARGE cohorts visual semi-quantitative rating scales were used to quantify PVS burden. As different scales were used across studies we dichotomized PVS burden into “extensive PVS burden” versus the rest in each cohort, defined by a cut-off closest to the top quartile of the semi-quantitative scale distribution (**Supplementary Appendix, Supplementary Table 2)**. In the Rotterdam Study III (RSIII) and in UKB a novel automated method was used to detect the number of PVS.[30] We dichotomized PVS burden in RSIII and UKB using the top quartile as the cut-off.

Covariates and descriptive variables

Total intracranial volume was available in all studies except ASPS, and was defined as the sum of grey matter, white matter and CSF volumes. Brain parenchymal fraction was used in ASPS and defined as the ratio of brain parenchymal tissue volume to total volume within the surface contour of the whole brain. Other covariates are described in the **Supplementary Methods**.

Genotyping and imputation

Genome wide genotypes were imputed to the 1000 Genomes project (1000G) phase I v3 or the Haplotype Reference Consortium (HRC) reference panels (**Supplementary Table 3**).

PVS genome-wide-association analyses in individual cohorts

Ancestry-specific logistic regression analyses with an additive genetic model were performed, adjusting for age, sex, and total intracranial volume (or brain parenchymal fraction for ASPS), relevant principal components of population stratification, and study site.

PVS genome-wide-association meta-analyses

First we performed quality control (QC) in each study following recommendations of Winkler et al.[101] Analyses were done on autosomal biallelic markers. Duplicate markers were removed, marker names and alleles were harmonized across studies, and P-Z plots (to check if the erroneous p-values are removed), quantile-quantile (QQ) plots and allele frequency-plots were constructed. In each study rare variants (minor allele frequency (MAF) < 0.01), variants with low imputation accuracy (R^2, oevar_imp or info score < 0.5) and extensive effect size values ($\beta > 5$ or $\beta < -5$) were removed. The number of SNPs passing QC for each study is reported in **Supplementary Table 4**. In stage 1 we conducted a GWAS meta-analysis of all CHARGE cohorts. First, a sample size weighted meta-analysis was conducted in each ancestry group (European (EUR), Asian (ASN), African-American (AA), Hispanics (HISP)) using METAL, followed by a meta-analysis across ancestries.[102] Genomic control was applied to each study-specific GWAS with a genomic inflation factor greater than 1.00. The effective allele count was defined as twice the product of the MAF, imputation accuracy and number of participants with extensive PVS. Variants with an effective allele count < 10 were excluded from the meta-analysis. So were variants with significant heterogeneity (Phet < 5.0×10^{-8}). We performed LD clumping, sorting the genome-wide significant SNPs by p-value, keeping the most significant SNP and removing SNPs with an $r^2>0.1$ within 1 Mb. Only variants present in at least half of the participants of the final meta-analysis were used to construct QQ and Manhattan plots. All genome-wide significant associations identified in CHARGE were tested for follow-up in the independent UKB sample (N=28,500). In stage 2 we conducted a combined meta-analysis of CHARGE and UKB cohorts using sample size weighted meta-analysis with METAL. We first meta-analyzed the UKB GWAS with European ancestry CHARGE cohorts and then combined GWAS across ancestries as in stage 1.

PVS next generation sequencing association analyses

Using recently released whole exome sequencing (WES) data from 16,955 UKB participants and the whole exome component of the whole genome sequencing data from the BRIDGET consortium (N=2,015, **Supplementary Methods**), we performed a meta-analysis of whole exome association studies (WEAS) of PVS burden. The next generation sequencing (NGS) data processing and QC is described in the **Supplementary Methods**. We used the REGENIE software[103] to perform single variant association tests of all exonic variants and gene-based burden tests of protein modifying rare variants individually in UKB and BRIDGET data. We combined results from UKB and BRIDGET using inverse-variance weighted meta-analysis implemented in the METAL software.[102] A logistic regression score adjusted for age, sex, and total intracranial volume was used to test association between a genetic marker and extensive PVS burden in BG, WM and HIP. To account for the imbalanced case-control ratio REGENIE by default implements the Firth correction when the logistic regression score test derived p-value is less than 0.05. For single variant association testing, we removed variants with a minor allele count < 5. For gene-based burden tests of protein modifying rare variants we considered variants annotated to be a splice acceptor, splice donor, start lost, stop lost, stop gained, frameshift, inframe insertion, inframe deletion, or missense by variant effect predictor (VEP, v90) software with MAF<0.01. We used the 'comphet' scheme in the REGENIE software, which thresholds the maximum number of rare alleles in a gene in individual samples to 2, to perform gene-based burden tests.

Conditional and joint multiple-SNP analysis

We used Genome-wide Complex Trait Analysis (GCTA)-COJO to perform conditional and joint multiple-SNP analysis of PVS GWAS summary statistics, with LD correction between SNPs, to identify secondary association signals at each of the genome-wide significant loci within 1 Mb of the lead SNP. This method relied on a stepwise selection procedure to select SNPs based on the conditional p-values, and the joint effects of all selected SNPs after optimization of the model was estimated.[31] We used the 1000 Genomes imputed 3C-Dijon study data for LD correction.

Trans-ethnic meta-regression of genome-wide association studies

We conducted a multi-ancestry meta-analysis using the MR-MEGA software,[104] which uses meta-regression to model allelic effects including axes of genetic variation as covariates in the model.

Gene based analysis

We performed gene-based analyses on European PVS GWAS meta-analysis. First we used the Multi-marker Analysis of GenoMic Annotation (MAGMA) software[32] implemented in FUMA[105] to perform a gene-based association study including 19,037 protein coding genes. This method is based on a multiple linear principal components regression model. We included variants located within 10kb of the 3' and 5' UTRs of a gene to include regulatory variants. Gene-wide significance was defined at $p<2.63x10^{-6}$. We also performed gene-based tests using the VEGAS2 software,[33] including 18,371 autosomal genes, leading to a gene-wide significance at $p<2.72x10^{-6}$. We included variants located within 10kb of the 3' and 5' UTRs of a gene to capture regulatory variants. Genes were considered in the same locus if they were <200kb of each other.

PVS heritability estimates

We used LD-score regression (ldsc package https://github.com/bulik/ldsc/) to estimate the heritability of extensive PVS burden in each location.

Multitrait analysis of PVS GWAS with GWAS of other MRI-markers of cSVD

We conducted a joint analysis of summary statistics from GWAS of PVS, WMH and lacunes with a Multi-Trait Analysis of GWAS (MTAG).[34] Because of the genetic correlation between these MRI-markers of cSVD, we expected to gain in power with MTAG by incorporating information contained in the GWAS estimates for the other MRI-markers of cSVD. MTAG results are obtained after estimating the variance-covariance matrix of the GWAS estimation error using LD score regression and the variance-covariance matrix of the SNP effects using method of moments. The MTAG method is based on a generalized model and the MTAG estimator is a weighted sum of the GWAS estimates. Of all genome-wide significant risk variants for PVS burden resulting from the MTAG analysis, only variants with a p-value < 0.05 in the univariate PVS GWAS and showing greater significance in MTAG than in univariate analyses for PVS, WMH, and lacunes were prioritized.

Analysis of associations findings across the age and disease spectrum

We searched for an association of WM and BG PVS genome-wide significant loci identified in the GWAS with extensive PVS burden in 1,748 young adults aged 22.1±2.3 years, participating in the i-Share study. We also constructed a weighted genetic risk score (wGRS) of WM PVS burden, including the 21 independent SNPs identified in the European GWAS (r^2<0.10 based on the 1000G European reference panel), weighted by the effects of the SNPs in the GWAS, the effect allele being the allele associated with increased PVS burden; the wGRS was rescaled (rwGRS) so that one unit of the genetic risk score corresponds to one additional WM PVS risk allele. We tested the association of this rwGRS with WM PVS burden in i-Share using logistic regression, adjusted for sex, age at MRI, intracranial volume and the first four principal components of population stratification.

Meta-regression with age

We tested for a significant modifying effect of age on associations with WM PVS for the three genome-wide significant WM PVS loci that also showed significant associations with WM PVS in young adults. For this purpose we collected the effect estimates (along with their standard errors) for the lead SNPs at these three loci in each individual cohort. We fitted a meta-regression of the lead SNPs' effect sizes onto an intercept and age. Meta-regression analysis was performed using the Metafor package in R,[106] and any statistical evidence of linear association was corrected for multiple testing (Bonferroni correction), using $p<0.05/3=1.7x10^{-2}$.

Shared genetic variation with other phenotypes

To explore shared genetic variation with vascular and neurological phenotypes, analyses were conducted on the stage 2 European ancestry meta-analysis. These phenotypes included: (i) putative risk factors (SBP,[107] DBP,[107] pulse pressure (PP),[107] body mass index (BMI),[108] high density lipoprotein (HDL) cholesterol,[109] low density lipoprotein (LDL) cholesterol,[109] triglycerides,[109] type 2 diabetes,[110] and sleep patterns);[111] (ii) other MRI-markers of brain aging (WMH burden,[10] covert MRI-defined brain infarcts and lacunes,[35] and hippocampal,[112] accumbens, amygdala, caudate, pallidum and putamen volumes);[113] and (iii) the most common neurological conditions previously reported to be associated with PVS, namely stroke (any stroke, any ischemic stroke, large artery stroke, cardio-embolic stroke, small vessel stroke,[114] intracerebral hemorrhage [ICH]),[115] AD,[116] and Parkinson disease.[117]

Summary statistics of the largest publicly available GWAS were obtained. To decrease the potential bias due to poor imputation quality, the summary statistics were filtered to the subset of HapMap 3 SNPs for each trait.

First, we explored whether genome-wide significant PVS risk loci (lead variants or variants in linkage disequilibrium with $r^2>0.9$, based on the 1000G European reference panel) were associated with these traits. A p-value threshold $<7.9x10^{-4}$ correcting for 21 independent phenotypes and for the 3 PVS locations was used (**Supplementary Methods**).

Second, we used LD-score regression (ldsc package https://github.com/bulik/ldsc/) to estimate the genetic correlation of extensive PVS burden with these phenotypes (again $p<7.9x10^{-4}$ was used as a significance threshold).

Mendelian randomization

We used a Mendelian randomization approach to explore the causal relation of putative risk factors (SBP, DBP, PP, BMI, LDL- and HDL-cholesterol, triglycerides, type 2 diabetes, and sleep patterns) with extensive PVS burden, and of extensive PVS burden with neurological traits (stroke, AD and Parkinson diseases).

First we used the Generalised Summary-data-based Mendelian randomisation (MR)method implemented in the GCTA software (GCTA-GSMR).[40] This method was based on a generalized least squares approach using genome-wide significant SNPs associated with the exposure ($p<5x10^{-8}$) as an instrument (**Supplementary Methods**). The heterogeneity in independent instrument (HEIDI)-outlier method was used to remove SNPs from genetic instruments that showed pleiotropic effects on both the exposure and the outcome. A $p<1.19x10^{-3}$ correcting for 14 independent phenotypes and the 3 PVS locations was considered significant. Only results based on instruments with at least 10 SNPs are shown (leading to the exclusion of instruments for BG and HIP PVS).

Second, for significant GSMR associations we conducted a secondary MR analysis using RadialMR,[41] to estimate the putative causal effect (β_{IVW}) of an exposure on the outcome using the inverse-variance weighting (IVW) method (**Supplementary Methods**).[41,118] Cochran's Q statistic was used to test for the presence of heterogeneity ($p<0.05$) due to horizontal pleiotropy that occurs when instruments affect the outcome independently of the exposure.[41] Outlier SNPs were identified by regressing the predicted causal estimate against the inverse variance weights and excluded. We then re-ran IVW tests, as well as MR-Egger regression,[119] assessing heterogeneity using the Rücker's Q' statistic.[41] We calculated the Q_R statistic as the ratio of Q' (Egger) on Q (IVW). A Q_R close to 1 indicates that both IVW and MR-Egger models fit the data equally well and made us select the IVW model. Finally, we formally ruled out horizontal pleiotropy by not interpreting the results for models with a significant MR-Egger intercept ($p<0.05$). Results from the IVW fixed effect estimates from RadialMR are also presented.[41]

To account for potential residual correlated pleiotropy and confirm the significant associations we identified using GSMR and RadialMR, we used MR-CAUSE (Causal Analysis Using Summary Effect Estimates).[120] MR-CAUSE compares two models (a "sharing" model allowing for horizontal pleiotropy but no causal effect, and a "causal" model estimating the putative causal effect of the exposure on the outcome) using the expected log pointwise posterior density (ELPD) by producing a one-sided p-value testing that the sharing model fits the data at least as well as the causal model: when this p-value was <0.05 we concluded that there were no evidence for correlated pleiotropy and thus that a causal effect seemed plausible.[120]

Pathway analyses

We conducted pathway analyses on European PVS summary statistics, and used the 1000G phase 3 reference panel. We used MAGMA gene set analyses[32] implemented in FUMA[105] to identify pathways overrepresented in the associations. We identified genes associated with extensive PVS burden and estimated the correlation between genes, reflecting the LD between genes. The p-values and gene correlation matrix were used in a generalized least squares model. A p-value $<3.2x10^{-6}$ correction for 15,496 gene sets was considered significant. As a sensitivity analysis, we used the VEGAS2Pathway approach, which aggregates association strengths of individual markers into pre-specified biological pathways using VEGAS-derived gene association p-values for extensive PVS burden. The empirical significance threshold for VEGAS2Pathway was $1x10^{-5}$ accounting for 6,213 correlated pathways.[121]

GWAS catalog

We used the Functional Mapping and Annotation of Genome-Wide Association Studies (FUMA GWAS) platform to obtain extensive functional annotation for genome-wide significant SNPs.[105] We identified, among the genome-wide significant risk variants for extensive PVS, SNPs that were associated with another trait from the GWAS catalog at genome-wide significance.[38]

Enrichment analyses in OMIM and COSMIC genes

Using a hypergeometric test we performed enrichment analyses of genes within 1 Mb, 100 kb or 10 kb of the lead variants, but also of genes within 10 kb of the lead variants with intragenic variants, and genes within 10 kb of the genetic loci with intragenic lead variants. We used the rest of the protein-coding genome as reference. We performed the analysis first combining the loci of the 3 PVS locations, and second including only WM PVS burden loci. We searched for an enrichment in different genes groups from the Online Mendelian Inheritance in Man (OMIM) database,[122] including perivascular spaces *("perivascular space" OR "virchow-robin space"*), white matter hyperintensities (*leukoaraiosis OR "white matter lesion" OR "white matter hyperintensities"*) and leukodystrophy (*leukodystrophy OR leukoencephalopathy*) genes. We also searched for an enrichment of genes involved in glioma and glioblastoma identified in the catalogue of somatic mutations in cancer (COSMIC, https://cancer.sanger.ac.uk).[123]

Transcriptome-wide association study

We performed transcriptome-wide association studies (TWAS) using TWAS-Fusion[47] to identify genes whose expression is significantly associated with PVS burden without directly measuring expression levels. We restricted the analysis to tissues considered relevant for cerebrovascular disease, and used precomputed functional weights (primarily gene expression) from 22 publicly available gene expression reference panels from blood, arterial, brain and peripheral nerve tissues (**Supplementary Methods**). Through imputation of gene expression we estimated the correlation between the genetic component of expression and the genetic component of PVS burden. Transcriptome-wide significant genes (eGenes) and the corresponding QTLs (eQTLs) were determined using Bonferroni correction (p-value $<3.93x10^{-6}$, **Supplementary Methods**). When a locus is highly significant and LD is extensive, association statistics may be inflated by chance QTL colocalization. We conducted a conditional analysis to identify significant expression-trait associations (or genetic correlation between expression and trait) after conditioning on the GWAS statistics (SNP-trait effects) at the locus with a permutation test. Associations with a p-value <0.05 were considered significant. Then we performed a genetic colocalization analysis of gene expression and PVS burden at each significant TWAS loci using the COLOC R package,[124] based on a Bayesian framework, in order to identify shared genetic causal variants (posterior probability PP4 $\geq$0.75) between the gene expression and the trait. This method is. Gene regions with eQTLs not reaching genome-wide significance in

association with PVS, and not in LD (r^2<0.01) with the lead SNP for genome-wide significant PVS risk loci, were considered as novel.

Cell type enrichment analysis

We conducted a cell-type enrichment analysis using **S**ingle cell **T**ype **E**nrichment **A**nalysis for **P**henotypes (https://github.com/erwinerdem/STEAP/). This is an extension to CELLECT and uses S-LDSC,[48] MAGMA,[32] and H-MAGMA[49] for enrichment analysis. PVS GWAS summary statistics were first munged. Then, expression specificity profiles were calculated using human and mouse single cell RNA-seq databases (**Supplementary Table 22**). Cell-type enrichment was calculated with three models : MAGMA, H-MAGMA (incorporating chromatin interaction profiles from human brain tissues in MAGMA) and stratified LD score regression. P-values were corrected for the number of independent cell-types in each database (Bonferroni correction).

Enrichment in drug target genes

We used the GREP (Genome for Repositioning)[53] software tool that quantifies an enrichment of gene sets from GWAS summary statistics in drugs of certain ATC classes or indicated for some ICD10 disease categories and captures potentially repositionable drugs targeting the gene set. Genes significantly detected (FDR-q <0.1) in MAGMA software were used for enrichment analyses in GREP software with the target genes of approved or investigated drugs curated in DrugBank and Therapeutic Target Database.

We used the Trans-Phar (integration of TWAS and Pharmacological database) software to identify drug target candidates in a specific tissue or cell-type category.[54] First a TWAS using FOCUS, which demonstrates fine-mapping of causal gene sets from TWAS results, and 27 tissues in GTEx v7 database (corresponding to defined 13 tissue-cell-type categories assigned by the 27 tissues in GTEx v7 database and 77 LINCS CMap L1000 library cell types) was performed to identify up- and down-regulated genes in participants with extensive PVS burden, and select the top 10% genes with the highest expression variation. Then we performed a negative Spearman's rank correlation analysis between the top 10% genes expression (Z-score) and the LINCS CMap L1000 library database.

Lifetime brain gene expression profile

We studied the lifetime expression of the genes identified in the TWAS and GWAS analyses, and the 3 genes associated with WM PVS burden in both the old and young populations to search for developmental processes. We used a public database https://hbatlas.org/ comprising genome-wide exon-level transcriptome data from 1,340 tissue samples from 16 brain regions (cerebellar cortex, mediodorsal nucleus of the thalamus, striatum, amygdala, hippocampus, and 11 areas of the neocortex) of 57 postmortem human brains, from embryonic development to late adulthood men and women of different ancestries. Donors were genotyped using an Illumina 2.5 million SNP chip, and transcriptome data was obtained using total RNA extracted with Illumina 2.5 million SNP chip, with stringent quality control criteria.[51]

Declarations

Acknowledgements

Detailed acknowledgements are included in the **Supplementary Appendix.** We thank all the participating cohorts for contributing to this study. We thank Dr. Judith Thomas-Crusells for editorial assistance.

Author contributions

C.T., J.M.W., S.Seshadri, H.H.H.A., and S.D. jointly supervised research. M-G.D., M.J.K., Q.LG., T.E.E. and A.M. contributed equally. M-G.D., M.J.K., H.H.H.A. and S.D. designed and conceived the study. J.R.R., S.F., M.L., E.H., M.B., N.D.D., P.D., S.H., R.M.T., F.D., J.S., Y.S., N.J.A., C.B., M.E.B., A.B., H.B., R.B., C.C., C.Chen, C-Y.C, I.J.D., P.G.G., J.J.H., J.J., S. L., M.M., P.M., Z.M., S.M-M., M.P., P.P., T.R., M.S., S.S., A.T., A.Thalamuthu, J.N.T., A.Tsuchida, M.C.V-H, M.W.V., U.V., K.W., T.Y.W., M.J.W., Q.Y., J.Z., W.Z., Y.Z., H.S., P.S.S., W.W., C.L.S., R.L. S., M.Lathrop., I.F-C., B.M., H.J.G., K.A.M., R.S. and M.A.I. generated the PVS phenotype, genomic data and conducted cohort-wise GWAS analyses. G.R., T.K., D-A.T., A.J.,T.P. and Y.O. contributed to bioinformatics analyses. M-G.D., M.J.K., Q.LG., T.E.E., A.M., C.T., J.M.W., S.Seshadri, H.H.A., and S.D. wrote and edited the manuscript.

Data availability

Genome-wide summary statistics generated and analyzed during the current study are deposited in a public repository (https://www.ncbi.nlm.nih.gov/gap/). All other data supporting the findings of this study are available either within the article, the supplementary information and supplementary data files, or from the authors upon reasonable request.

Competing interests

The authors declared no potential conflicts of interest with respect to research, authorship, and/or publication of this article.

References

1. Pollock, H., Hutchings, M., Weller, R.O. & Zhang, E.T. Perivascular spaces in the basal ganglia of the human brain: their relationship to lacunes. *J Anat* **191** (**Pt 3**), 337–346 (1997).
2. Zhang, E.T., Inman, C.B. & Weller, R.O. Interrelationships of the pia mater and the perivascular (Virchow-Robin) spaces in the human cerebrum. *Journal of Anatomy* **170**, 111–123 (1990).
3. Wardlaw, J.M., *et al.* Perivascular spaces in the brain: anatomy, physiology and pathology. *Nat Rev Neurol* **16**, 137–153 (2020).
4. Mestre, H., Kostrikov, S., Mehta, R.I. & Nedergaard, M. Perivascular spaces, glymphatic dysfunction, and small vessel disease. *Clin Sci (Lond)* **131**, 2257–2274 (2017).
5. Jessen, N.A., Munk, A.S.F., Lundgaard, I. & Nedergaard, M. The Glymphatic System: A Beginner's Guide. *Neurochemical Research* **40**, 2583–2599 (2015).
6. Yao, M., *et al.* Hippocampal perivascular spaces are related to aging and blood pressure but not to cognition. *Neurobiology of Aging* **35**, 2118–2125 (2014).
7. Zhu, Y.-C., *et al.* Severity of dilated Virchow-Robin spaces is associated with age, blood pressure, and MRI markers of small vessel disease: a population-based study. *Stroke* **41**, 2483–2490 (2010).
8. Potter, G.M., *et al.* Enlarged perivascular spaces and cerebral small vessel disease. *International Journal of Stroke* **10**, 376–381 (2015).
9. Wardlaw, J.M., *et al.* Neuroimaging standards for research into small vessel disease and its contribution to ageing and neurodegeneration. *The Lancet Neurology* **12**, 822–838 (2013).
10. Sargurupremraj, M., *et al.* Cerebral small vessel disease genomics and its implications across the lifespan. *Nat Commun* **11**, 6285 (2020).

11. Debette, S., Schilling, S., Duperron, M.G., Larsson, S.C. & Markus, H.S. Clinical Significance of Magnetic Resonance Imaging Markers of Vascular Brain Injury: A Systematic Review and Meta-analysis. *JAMA Neurol* **76**, 81–94 (2019).
12. Deramecourt, V., *et al.* Staging and natural history of cerebrovascular pathology in dementia. *Neurology* **78**, 1043–1050 (2012).
13. Bacyinski, A., Xu, M., Wang, W. & Hu, J. The Paravascular Pathway for Brain Waste Clearance: Current Understanding, Significance and Controversy. *Front Neuroanat* **11**, 101 (2017).
14. Xie, L., *et al.* Sleep drives metabolite clearance from the adult brain. *Science* **342**, 373–377 (2013).
15. Zhu, Y.C., *et al.* High degree of dilated Virchow-Robin spaces on MRI is associated with increased risk of dementia. *J Alzheimers Dis* **22**, 663–672 (2010).
16. Duperron, M.G., *et al.* High dilated perivascular space burden: a new MRI marker for risk of intracerebral hemorrhage. *Neurobiol Aging* **84**, 158–165 (2019).
17. Chen, W., Song, X. & Zhang, Y. Assessment of the Virchow-Robin Spaces in Alzheimer disease, mild cognitive impairment, and normal aging, using high-field MR imaging. *AJNR. American journal of neuroradiology* **32**, 1490–1495 (2011).
18. Ramirez, J., *et al.* Visible Virchow-Robin spaces on magnetic resonance imaging of Alzheimer's disease patients and normal elderly from the Sunnybrook Dementia Study. *J Alzheimers Dis* **43**, 415–424 (2015).
19. Martinez-Ramirez, S., *et al.* Perivascular Spaces Volume in Sporadic and Hereditary (Dutch-Type) Cerebral Amyloid Angiopathy. *Stroke* **49**, 1913–1919 (2018).
20. Roher, A.E., *et al.* Cortical and leptomeningeal cerebrovascular amyloid and white matter pathology in Alzheimer's disease. *Mol Med* **9**, 112–122 (2003).
21. Mestre, H., *et al.* Cerebrospinal fluid influx drives acute ischemic tissue swelling. *Science* **367**(2020).
22. Månberg, A., *et al.* Altered perivascular fibroblast activity precedes ALS disease onset. *Nat Med* **27**, 640–646 (2021).
23. Duperron, M.G., *et al.* Burden of Dilated Perivascular Spaces, an Emerging Marker of Cerebral Small Vessel Disease, Is Highly Heritable. *Stroke* (2018).
24. Zhang, C., *et al.* Risk factors of dilated Virchow-Robin spaces are different in various brain regions. *PLoS One* **9**, e105505 (2014).
25. Psaty, B.M., *et al.* Cohorts for Heart and Aging Research in Genomic Epidemiology (CHARGE) Consortium: Design of prospective meta-analyses of genome-wide association studies from 5 cohorts. *Circ Cardiovasc Genet* **2**, 73–80 (2009).
26. Potter, G.M., Chappell, F.M., Morris, Z. & Wardlaw, J.M. Cerebral perivascular spaces visible on magnetic resonance imaging: development of a qualitative rating scale and its observer reliability. *Cerebrovascular diseases* **39**, 224–231 (2015).
27. Riba-Llena, I., *et al.* Assessment of enlarged perivascular spaces and their relation to target organ damage and mild cognitive impairment in patients with hypertension. *Eur J Neurol* **23**, 1044–1050 (2016).
28. Adams, H.H., *et al.* Rating method for dilated Virchow-Robin spaces on magnetic resonance imaging. *Stroke* **44**, 1732–1735 (2013).
29. Gutierrez, J., *et al.* Pulsatile and steady components of blood pressure and subclinical cerebrovascular disease: the Northern Manhattan Study. *J Hypertens* **33**, 2115–2122 (2015).

30. Dubost, F., *et al.* Enlarged perivascular spaces in brain MRI: Automated quantification in four regions. *Neuroimage* **185**, 534–544 (2019).
31. Yang, J., *et al.* Conditional and joint multiple-SNP analysis of GWAS summary statistics identifies additional variants influencing complex traits. *Nat Genet* **44**, 369–375, S361-363 (2012).
32. de Leeuw, C.A., Mooij, J.M., Heskes, T. & Posthuma, D. MAGMA: generalized gene-set analysis of GWAS data. *PLoS Comput Biol* **11**, e1004219 (2015).
33. Mishra, A. & Macgregor, S. VEGAS2: Software for More Flexible Gene-Based Testing. *Twin Res Hum Genet* **18**, 86–91 (2015).
34. Turley, P., *et al.* Multi-trait analysis of genome-wide association summary statistics using MTAG. *Nat Genet* **50**, 229–237 (2018).
35. Chauhan, G., *et al.* Genetic and lifestyle risk factors for MRI-defined brain infarcts in a population-based setting. *Neurology* (2019).
36. Sveinbjornsson, G., *et al.* Weighting sequence variants based on their annotation increases power of whole-genome association studies. *Nat Genet* **48**, 314–317 (2016).
37. Tsuchida, A., *et al.* The MRi-Share database: brain imaging in a cross-sectional cohort of 1870 university students. *Brain Struct Funct* **226**, 2057–2085 (2021).
38. Buniello, A., *et al.* The NHGRI-EBI GWAS Catalog of published genome-wide association studies, targeted arrays and summary statistics 2019. *Nucleic Acids Res* **47**, D1005-D1012 (2019).
39. Bulik-Sullivan, B.K., *et al.* LD Score regression distinguishes confounding from polygenicity in genome-wide association studies. *Nat Genet* **47**, 291–295 (2015).
40. Zhu, Z., *et al.* Causal associations between risk factors and common diseases inferred from GWAS summary data. *Nat Commun* **9**, 224 (2018).
41. Bowden, J., *et al.* Improving the visualization, interpretation and analysis of two-sample summary data Mendelian randomization via the Radial plot and Radial regression. *Int J Epidemiol* **47**, 1264–1278 (2018).
42. van der Knaap, M.S., Schiffmann, R., Mochel, F. & Wolf, N.I. Diagnosis, prognosis, and treatment of leukodystrophies. *Lancet neurology* **18**, 962–972 (2019).
43. Sosunov, A., Olabarria, M. & Goldman, J.E. Alexander disease: an astrocytopathy that produces a leukodystrophy. *Brain pathology (Zurich, Switzerland)* **28**, 388–398 (2018).
44. Dewulf, J.P., *et al.* SLC13A3 variants cause acute reversible leukoencephalopathy and α-ketoglutarate accumulation. *Ann Neurol* **85**, 385–395 (2019).
45. Pennisi, A., *et al.* Heterogeneity of PNPT1 neuroimaging: mitochondriopathy, interferonopathy or both? *Journal of medical genetics* (2020).
46. Bamborschke, D., *et al.* PNPT1 mutations may cause Aicardi-Goutières-Syndrome. *Brain & development* **43**, 320–324 (2021).
47. Gusev, A., *et al.* Integrative approaches for large-scale transcriptome-wide association studies. *Nat Genet* **48**, 245–252 (2016).
48. Finucane, H.K., *et al.* Partitioning heritability by functional annotation using genome-wide association summary statistics. *Nat Genet* **47**, 1228–1235 (2015).
49. Sey, N.Y.A., *et al.* A computational tool (H-MAGMA) for improved prediction of brain-disorder risk genes by incorporating brain chromatin interaction profiles. *Nat Neurosci* **23**, 583–593 (2020).

50. Cao, J., *et al.* A human cell atlas of fetal gene expression. *Science* **370**(2020).
51. Kang, H.J., *et al.* Spatio-temporal transcriptome of the human brain. *Nature* **478**, 483–489 (2011).
52. Okada, Y., *et al.* Genetics of rheumatoid arthritis contributes to biology and drug discovery. *Nature* **506**, 376–381 (2014).
53. Sakaue, S. & Okada, Y. GREP: genome for REPositioning drugs. *Bioinformatics* **35**, 3821–3823 (2019).
54. Konuma, T., Ogawa, K. & Okada, Y. Integration of genetically regulated gene expression and pharmacological library provides therapeutic drug candidates. *Hum Mol Genet* **30**, 294–304 (2021).
55. Joutel, A., Haddad, I., Ratelade, J. & Nelson, M.T. Perturbations of the cerebrovascular matrisome: A convergent mechanism in small vessel disease of the brain? *J Cereb Blood Flow Metab* **36**, 143–157 (2016).
56. Traylor, M., *et al.* Genetic basis of lacunar stroke: a pooled analysis of individual patient data and genome-wide association studies. *Lancet neurology* (2021).
57. Persyn, E., *et al.* Genome-wide association study of MRI markers of cerebral small vessel disease in 42,310 participants. *Nat Commun* **11**, 2175 (2020).
58. Hara, K., *et al.* Association of HTRA1 mutations and familial ischemic cerebral small-vessel disease. *N Engl J Med* **360**, 1729–1739 (2009).
59. Simon, A.J., *et al.* Mutations in STN1 cause Coats plus syndrome and are associated with genomic and telomere defects. *The Journal of experimental medicine* **213**, 1429–1440 (2016).
60. Wardlaw, J.M., Smith, C. & Dichgans, M. Mechanisms of sporadic cerebral small vessel disease: insights from neuroimaging. *The Lancet. Neurology* **12**, 483–497 (2013).
61. Piantino, J., *et al.* Characterization of MR Imaging-Visible Perivascular Spaces in the White Matter of Healthy Adolescents at 3T. *AJNR. American journal of neuroradiology* **41**, 2139–2145 (2020).
62. Rajani, R.M., *et al.* Reversal of endothelial dysfunction reduces white matter vulnerability in cerebral small vessel disease in rats. *Science Translational Medicine* **10**, eaam9507 (2018).
63. Carelli, V., *et al.* Syndromic parkinsonism and dementia associated with OPA1 missense mutations. *Ann Neurol* **78**, 21–38 (2015).
64. Backhouse, E., *et al.* Early life predictors of late life cerebral small vessel disease in four prospective cohort studies. *Brain* (2021 in press (MEDRXIV/2021/252900)).
65. Yung, Y.C., Stoddard, N.C. & Chun, J. LPA receptor signaling: pharmacology, physiology, and pathophysiology. *Journal of lipid research* **55**, 1192–1214 (2014).
66. Plastira, I., *et al.* MAPK signaling determines lysophosphatidic acid (LPA)-induced inflammation in microglia. *J Neuroinflammation* **17**, 127 (2020).
67. Crack, P.J., *et al.* Anti-lysophosphatidic acid antibodies improve traumatic brain injury outcomes. *J Neuroinflammation* **11**, 37 (2014).
68. Weiner, J.A., Hecht, J.H. & Chun, J. Lysophosphatidic acid receptor gene vzg-1/lpA1/edg-2 is expressed by mature oligodendrocytes during myelination in the postnatal murine brain. *The Journal of comparative neurology* **398**, 587–598 (1998).
69. Mollink, J., *et al.* The spatial correspondence and genetic influence of interhemispheric connectivity with white matter microstructure. *Nat Neurosci* **22**, 809–819 (2019).
70. Gaire, B.P., Sapkota, A., Song, M.R. & Choi, J.W. Lysophosphatidic acid receptor 1 (LPA1) plays critical roles in microglial activation and brain damage after transient focal cerebral ischemia. *J Neuroinflammation* **16**, 170

(2019).

71. Gross, I. & Brauer, A.U. Modulation of lysophosphatidic acid (LPA) receptor activity: the key to successful neural regeneration? *Neural Regen Res* **15**, 53–54 (2020).
72. Hisaoka-Nakashima, K., *et al.* Mirtazapine increases glial cell line-derived neurotrophic factor production through lysophosphatidic acid 1 receptor-mediated extracellular signal-regulated kinase signaling in astrocytes. *Eur J Pharmacol* **860**, 172539 (2019).
73. Allanore, Y., *et al.* Lysophosphatidic Acid Receptor 1 Antagonist SAR100842 for Patients With Diffuse Cutaneous Systemic Sclerosis: A Double-Blind, Randomized, Eight-Week Placebo-Controlled Study Followed by a Sixteen-Week Open-Label Extension Study. *Arthritis Rheumatol* **70**, 1634–1643 (2018).
74. Stenman, J.M., *et al.* Canonical Wnt signaling regulates organ-specific assembly and differentiation of CNS vasculature. *Science* **322**, 1247–1250 (2008).
75. Chavali, M., *et al.* Wnt-Dependent Oligodendroglial-Endothelial Interactions Regulate White Matter Vascularization and Attenuate Injury. *Neuron* **108**, 1130-1145.e1135 (2020).
76. Capone, C., *et al.* Reducing Timp3 or vitronectin ameliorates disease manifestations in CADASIL mice. *Ann Neurol* **79**, 387–403 (2016).
77. Tanaka, T., *et al.* Plasma proteomic signatures predict dementia and cognitive impairment. *Alzheimers Dement (N Y)* **6**, e12018 (2020).
78. Jakobsson, L., Domogatskaya, A., Tryggvason, K., Edgar, D. & Claesson-Welsh, L. Laminin deposition is dispensable for vasculogenesis but regulates blood vessel diameter independent of flow. *FASEB journal: official publication of the Federation of American Societies for Experimental Biology* **22**, 1530–1539 (2008).
79. Yao, Y., Chen, Z.L., Norris, E.H. & Strickland, S. Astrocytic laminin regulates pericyte differentiation and maintains blood brain barrier integrity. *Nat Commun* **5**, 3413 (2014).
80. Menezes, M.J., *et al.* The extracellular matrix protein laminin α2 regulates the maturation and function of the blood-brain barrier. *The Journal of Neuroscience: The Official Journal of the Society for Neuroscience* **34**, 15260–15280 (2014).
81. Chung, J., *et al.* Genome-wide association study of cerebral small vessel disease reveals established and novel loci. *Brain* **142**, 3176–3189 (2019).
82. Armstrong, N.J., *et al.* Common Genetic Variation Indicates Separate Causes for Periventricular and Deep White Matter Hyperintensities. *Stroke* **51**, 2111–2121 (2020).
83. Hadano, S., *et al.* A gene encoding a putative GTPase regulator is mutated in familial amyotrophic lateral sclerosis 2. *Nat Genet* **29**, 166–173 (2001).
84. Bindesbøll, C., *et al.* NBEAL1 controls SREBP2 processing and cholesterol metabolism and is a susceptibility locus for coronary artery disease. *Sci Rep* **10**, 4528 (2020).
85. Beyens, A., *et al.* Arterial tortuosity syndrome: 40 new families and literature review. *Genetics in medicine: official journal of the American College of Medical Genetics* **20**, 1236–1245 (2018).
86. Pico, F., Labreuche, J., Touboul, P.J., Leys, D. & Amarenco, P. Intracranial arterial dolichoectasia and small-vessel disease in stroke patients. *Ann Neurol* **57**, 472–479 (2005).
87. Chen, Y.C., *et al.* Correlation Between Internal Carotid Artery Tortuosity and Imaging of Cerebral Small Vessel Disease. *Front Neurol* **11**, 567232 (2020).
88. Wang, C., *et al.* Mutations in SLC20A2 link familial idiopathic basal ganglia calcification with phosphate homeostasis. *Nat Genet* **44**, 254–256 (2012).

89. Ho, H.T., Dahlin, A. & Wang, J. Expression Profiling of Solute Carrier Gene Families at the Blood-CSF Barrier. *Frontiers in pharmacology* **3**, 154 (2012).
90. Wang, H., *et al.* Structure, function, and genomic organization of human Na(+)-dependent high-affinity dicarboxylate transporter. *American journal of physiology. Cell physiology* **278**, C1019-1030 (2000).
91. Wang, W.W., Gallo, L., Jadhav, A., Hawkins, R. & Parker, C.G. The Druggability of Solute Carriers. *Journal of medicinal chemistry* **63**, 3834–3867 (2020).
92. Lin, L., Yee, S.W., Kim, R.B. & Giacomini, K.M. SLC transporters as therapeutic targets: emerging opportunities. *Nature reviews. Drug discovery* **14**, 543–560 (2015).
93. Yang, S., *et al.* The relationship between ambulatory blood pressure variability and enlarged perivascular spaces: a cross-sectional study. *BMJ Open* **7**, e015719 (2017).
94. Mestre, H., *et al.* Flow of cerebrospinal fluid is driven by arterial pulsations and is reduced in hypertension. *Nat Commun* **9**, 4878 (2018).
95. Del Brutto, O.H., Mera, R.M., Del Brutto, V.J. & Castillo, P.R. Enlarged basal ganglia perivascular spaces and sleep parameters. A population-based study. *Clinical neurology and neurosurgery* **182**, 53–57 (2019).
96. Aribisala, B.S., *et al.* Sleep and brain morphological changes in the eighth decade of life. *Sleep Medicine* **65**, 152–158 (2020).
97. Shi, G., *et al.* A Rare Mutation of β(1)-Adrenergic Receptor Affects Sleep/Wake Behaviors. *Neuron* **103**, 1044-1055.e1047 (2019).
98. Chen, Z.L., *et al.* Ablation of astrocytic laminin impairs vascular smooth muscle cell function and leads to hemorrhagic stroke. *The Journal of cell biology* **202**, 381–395 (2013).
99. Rannikmäe, K., *et al.* COL4A2 is associated with lacunar ischemic stroke and deep ICH: Meta-analyses among 21,500 cases and 40,600 controls. *Neurology* **89**, 1829–1839 (2017).
100. Ballerini, L., *et al.* Computational quantification of brain perivascular space morphologies: Associations with vascular risk factors and white matter hyperintensities. A study in the Lothian Birth Cohort 1936. *NeuroImage. Clinical* **25**, 102120 (2020).
101. Winkler, T.W., *et al.* Quality control and conduct of genome-wide association meta-analyses. *Nat Protoc* **9**, 1192–1212 (2014).
102. Willer, C.J., Li, Y. & Abecasis, G.R. METAL: fast and efficient meta-analysis of genomewide association scans. *Bioinformatics* **26**, 2190–2191 (2010).
103. Mbatchou, J., *et al.* Computationally efficient whole-genome regression for quantitative and binary traits. *Nat Genet* (2021).
104. Magi, R., *et al.* Trans-ethnic meta-regression of genome-wide association studies accounting for ancestry increases power for discovery and improves fine-mapping resolution. *Hum Mol Genet* **26**, 3639–3650 (2017).
105. Watanabe, K., Taskesen, E., van Bochoven, A. & Posthuma, D. Functional mapping and annotation of genetic associations with FUMA. *Nat Commun* **8**, 1826 (2017).
106. Viechtenbauer, W. Conducting meta-analysis in R with the metafor Package. *J Stat Software* **36**(**3**): **1**-**48**.(2010).
107. Evangelou, E., *et al.* Genetic analysis of over 1 million people identifies 535 new loci associated with blood pressure traits. *Nat Genet* **50**, 1412–1425 (2018).
108. Yengo, L., *et al.* Meta-analysis of genome-wide association studies for height and body mass index in approximately 700000 individuals of European ancestry. *Hum Mol Genet* **27**, 3641–3649 (2018).

109. Willer, C.J., *et al.* Discovery and refinement of loci associated with lipid levels. *Nat Genet* **45**, 1274–1283 (2013).
110. Xue, A., *et al.* Genome-wide association analyses identify 143 risk variants and putative regulatory mechanisms for type 2 diabetes. *Nat Commun* **9**, 2941 (2018).
111. Dashti, H.S., *et al.* Genome-wide association study identifies genetic loci for self-reported habitual sleep duration supported by accelerometer-derived estimates. *Nat Commun* **10**, 1100 (2019).
112. Hibar, D.P., *et al.* Novel genetic loci associated with hippocampal volume. *Nat Commun* **8**, 13624 (2017).
113. Satizabal, C.L., *et al.* Genetic architecture of subcortical brain structures in 38,851 individuals. *Nat Genet* **51**, 1624–1636 (2019).
114. Malik, R., *et al.* Multiancestry genome-wide association study of 520,000 subjects identifies 32 loci associated with stroke and stroke subtypes. *Nat Genet* **50**, 524–537 (2018).
115. Woo, D., *et al.* Meta-analysis of genome-wide association studies identifies 1q22 as a susceptibility locus for intracerebral hemorrhage. *Am J Hum Genet* **94**, 511–521 (2014).
116. Schwartzentruber, J., *et al.* Genome-wide meta-analysis, fine-mapping and integrative prioritization implicate new Alzheimer's disease risk genes. *Nat Genet* **53**, 392–402 (2021).
117. Nalls, M.A., *et al.* Identification of novel risk loci, causal insights, and heritable risk for Parkinson's disease: a meta-analysis of genome-wide association studies. *Lancet neurology* **18**, 1091–1102 (2019).
118. Swerdlow, D.I., *et al.* Selecting instruments for Mendelian randomization in the wake of genome-wide association studies. *Int J Epidemiol* **45**, 1600–1616 (2016).
119. Bowden, J., Davey Smith, G. & Burgess, S. Mendelian randomization with invalid instruments: effect estimation and bias detection through Egger regression. *Int J Epidemiol* **44**, 512–525 (2015).
120. Morrison, J., Knoblauch, N., Marcus, J.H., Stephens, M. & He, X. Mendelian randomization accounting for correlated and uncorrelated pleiotropic effects using genome-wide summary statistics. *Nat Genet* **52**, 740–747 (2020).
121. Mishra, A. & MacGregor, S. A Novel Approach for Pathway Analysis of GWAS Data Highlights Role of BMP Signaling and Muscle Cell Differentiation in Colorectal Cancer Susceptibility. *Twin Res Hum Genet* **20**, 1–9 (2017).
122. Amberger, J.S., Bocchini, C.A., Schiettecatte, F., Scott, A.F. & Hamosh, A. OMIM.org: Online Mendelian Inheritance in Man (OMIM(R)), an online catalog of human genes and genetic disorders. *Nucleic Acids Res* **43**, D789-798 (2015).
123. Tate, J.G., *et al.* COSMIC: the Catalogue Of Somatic Mutations In Cancer. *Nucleic Acids Res* **47**, D941-D947 (2019).
124. Giambartolomei, C., *et al.* Bayesian test for colocalisation between pairs of genetic association studies using summary statistics. *PLoS Genet* **10**, e1004383 (2014).

Tables

Table 1. Genetic variants associated with high perivascular spaces burden

Region	SNP ALL	chr:position	EA/OA	EAF	Function	Nearest gene(s)	Z-score	Dir	N ext-PVS / total	p-val All Stage 1	p-val Follow-up	p-val EUR Stage 2	p-val All Stage 2	Het p-val
PVS in white matter														
20q13.12	rs6011998	20:45269867	C/T	0.95	intronic	*SLC13A3*	10.65	++++	9502/39128	**8.67E-08**	**3.36E-20**	**1.90E-24**	**1.80E-26**	0.11
3p25.1	rs13079464	3:13822439	C/G	0.46	intergenic	*WNT7A*	8.70	++++	9614/39822	**3.33E-09**	**5.66E-11**	**8.64E-17**	**3.41E-18**	0.59
20q13.12	rs2425884	20:45258292	C/T	0.57	intronic	*SLC13A3*	8.63	+-+-	9614/39822	8.09E-06	**1.46E-13**	**2.60E-18**	**6.02E-18**	0.14
9q31.3	rs10817108*	9:113658671	A/G	0.21	intronic	*LPAR1*	8.20	+++?	9550/39516	**8.35E-10**	**2.61E-09**	**1.07E-15**	**2.46E-16**	0.75
20q13.12	rs2425881	20:45255618	A/G	0.83	intronic	*SLC13A3*	7.68	+-+?	9496/39087	4.24E-05	**8.08E-11**	**2.02E-15**	**1.59E-14**	0.06
3q21.2	rs3772833	3:124518362	G/A	0.83	intronic	*ITGB5, UMPS*	7.67	+++?	9496/39087	1.37E-05	**2.49E-10**	**2.15E-13**	**1.76E-14**	0.39
20q13.12	rs112407396	20:45276381	T/A	0.03	intronic	*SLC13A3*	6.91	+???	8426/34530	2.14E-03	**5.85E-10**	**4.81E-12**	**4.81E-12**	1.00
1q41	rs10494988	1:215141570	C/T	0.63	intergenic	*CENPF,KCNK2*	6.54	++++	9614/39822	3.38E-05	**3.05E-07**	**2.23E-10**	**6.03E-11**	0.69
20q13.12	rs72485816†	20:45314435	T/C	0.96	UTR3	*TP53RK*	6.45	++?-	9114/37342	1.03E-02	**2.61E-09**	**1.47E-10**	**1.12E-10**	0.87
15q25.3	rs8041189	15:85686327	G/A	0.70	intergenic	*PDE8A*	6.44	+-??	9486/39315	9.78E-05	**2.50E-07**	**7.30E-11**	**1.24E-10**	0.31
3p25	rs4685022	3:13832611	G/A	0.65	intergenic	*WNT7A*	6.40	+++?	9576/39654	**3.89E-07**	**1.24E-05**	**2.36E-09**	**1.58E-10**	0.11
2p16.1	rs7596872	2:56128091	C/A	0.90	intronic	*EFEMP1*	6.31	+-??	9333/38442	1.33E-04	**3.95E-07**	**1.00E-10**	**2.80E-10**	0.11
17q21.31	rs1126642	17:42989063	C/T	0.96	exonic	*GFAP*	6.23	+?+?	9119/37466	1.41E-03	**8.67E-08**	**6.19E-10**	**4.67E-10**	0.72
3q29	rs687610†	3:193515781	G/C	0.43	intergenic	*OPA1*	6.20	+++-	9614/39822	2.79E-03	**5.36E-08**	**2.99E-10**	**5.81E-10**	0.76
6p25.2	rs4959689	6:2617122	C/A	0.58	intergenic	*C6orf195*	6.03	++++	9582/39695	3.16E-03	**1.38E-07**	**3.37E-09**	**1.63E-09**	1.00
20q13.12	rs56104388	20:45302135	T/C	0.99	intronic	*SLC13A3*	5.85	+???	7626/30916	6.23E-01	**2.61E-09**	**4.80E-09**	**4.80E-09**	1.00
11q13.3	rs12417836	11:70089700	T/C	0.07	intergenic	*FADD, PPFIA1*	5.58	+-+?	9464/38960	2.17E-04	**1.89E-05**	**1.56E-08**	**2.47E-08**	0.40
8p11.21	rs2923437†	8:42425399	A/C	0.41	intergenic	*SMIM19,CHRNB3, SLC20A2*	5.49	++--	9614/39822	2.77E-03	**4.22E-06**	**4.73E-08**	**4.08E-08**	0.14
6p25.3	rs1922930	6:1364691	C/A	0.12	intergenic	*FOXQ1,FOXF2*	5.47	++??	9406/38748	2.80E-02	**4.31E-07**	**3.60E-08**	**4.62E-08**	0.48
19p13.11	rs2385089	19:18550434	A/C	0.74	intergenic	*ISYNA1, ELL, LRRC25***	5.49	+++-	9614/39822	2.31E-02	**6.26E-07**	**4.14E-08**	5.73E-08	0.57
7q33	rs10954468	7:134434661	C/A	0.40	intergenic	*BPGM,CALD1***	5.52	+-?+	9524/39483	3.94E-02	**5.20E-07**	**3.39E-08**	8.79E-08	0.29
PVS in basal ganglia														
2q33.2	rs4675310†	2:203880834	A/G	0.87	intronic	*NBEAL1, ICA1L*	5.92	++??	9011/39243	3.71E-04	**1.93E-06**	**2.71E-09**	**3.27E-09**	0.64
3q26.31	rs6769442	3:171565463	G/A	0.75	intronic	*TMEM212*	5.74	++?+	9101/39788	5.35E-04	**4.06E-06**	**1.68E-08**	**9.34E-09**	0.96
PVS in hippocampus														
1q25.3	rs10797812†	1:182984597	A/G	0.54	intergenic	*SHCBP1L,LAMC1*	7.84	++++	9399/40095	1.70E-	**5.07E-**	**1.67E-**	**4.39E-**	0.68

2p16.1	rs78857879†	2:56135099	G/A	0.90	intronic	*EFEMP1*	6.43	+???	9033/38008	04 1.13E-02	**12** **2.61E-09**	**14** **8.20E-11**	**15** **1.31E-10**	1.00
1q41	rs6540873	1:215137222	A/C	0.62	intergenic	*CENPF,KCNK2*	5.95	+--+	9399/40095	9.31E-04	7.67E-07	**1.38E-09**	**2.72E-09**	0.11

PVS indicates perivascular spaces; EA, effective allele; EAF, effective allele frequency, N with ext-PVS correspond to the number of participants with extensive PVS burden in the combined meta-analysis; Het p-value corresponds to the heterogeneity p-value in the meta-analysis (combined stage 2 except for rs2385089 and rs10954468 for which the European stage 2 meta-analysis het p-value is reported); N total corresponds to the number of participants in the combined meta-analysis; dir corresponds to the association direction of the EA with the phenotype (extensive PVS burden versus the rest) for European, Hispanic, Asian, and African American ancestry studies, in this order; genome-wide significant loci (p-value<$5x10^{-8}$) are in bold; Z-scores of the combined sample size weighted meta-analysis (stage 2) are represented, except for the 2 SNPs reaching genome-wide significance in Europeans only (rs2385089, rs10954468) for which the European meta-analysis Z-score is reported. *corresponds to the top SNP of this locus in the combined meta-analysis (r >0.9 with the top SNP of this locus in the discovery meta-analysis); **Genome-wide significant association in Europeans only; †for these loci, the lead SNP was different in the European meta-analysis: rs72485816àrs6094423; rs687610àrs6444747; rs2923437à rs62509329; rs4675310à rs140244541; rs10797812à rs2022392; rs78857879à rs7596872; pvalue of the top SNP of this locus in the European meta-analysis (r >0.10 with the top SNP of this locus in the European meta-analysis).

Table 2. Association of WM PVS lead SNPs with WM PVS burden in the i-Share cohort (N=1,748)

Variables		Region	Nearest gene(s)	EA	OR (95%CI)	p-value
rwGRS *		**-**	-	-	1.11 (1.06-1.16)	2.62E-06
rs687610	3:193515781	3q29	*OPA1*	G	1.46 (1.18-1.81)	4.88E-04
rs7596872	2:56128091	2p16.1	*EFEMP1*	C	1.65 (1.09-2.49)	0.011
rs2425881	20:45255618	20q13.12	*SLC13A3*	A	1.46 (1.07-2.00)	0.014

CI: confidence interval; OR: odds ratio; rwGRS: rescaled weighted genetic risk score, for which the odds ratio corresponds to the increase in odds associated with each additional risk allele in the score; all analyses were adjusted for age, sex, total intracranial volume and the first 4 principal components of population stratification; *results were substantially unchanged after exclusion of 189 related and non-European participants (OR=1.12 [95%CI: 1.07-1.17], p=$2.63x10^{-6}$).

Figures

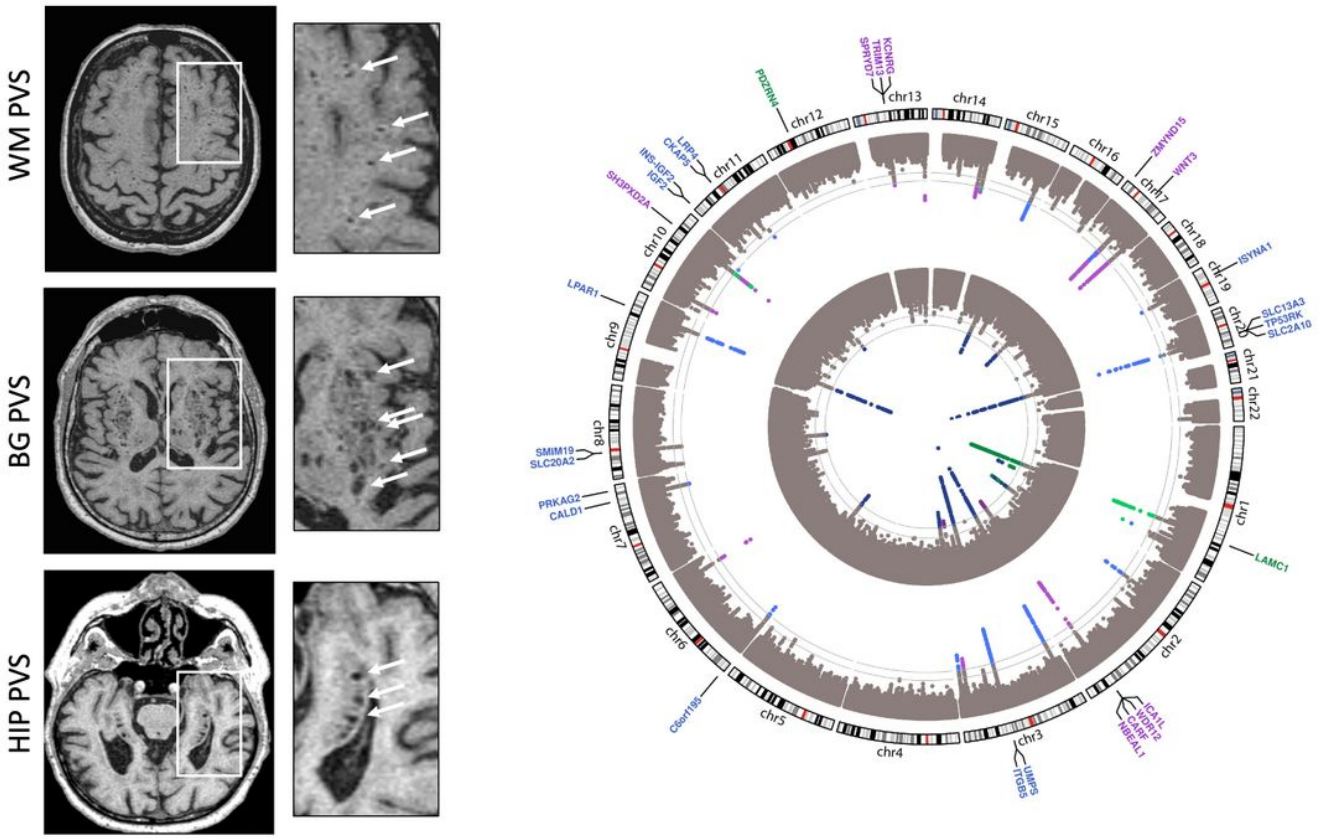

Figure 1

Illustration of extensive perivascular space burden and Manhattan plot of the PVS GWAS meta-analysis A. T1-weighted axial brain magnetic resonance images. Extensive perivascular space burden in basal ganglia (circles, top, BG PVS), white matter (arrows, middle, WM PVS), and hippocampus (arrows, bottom, HIP PVS) on T1-weighted axial magnetic resonance images; B. The inner circle corresponds to the GWAS results, the middle circle to MTAG results, and the outer circle to gene-based test results. Results for WM PVS are in blue, for BG PVS in purple and for HIP PVS in green.

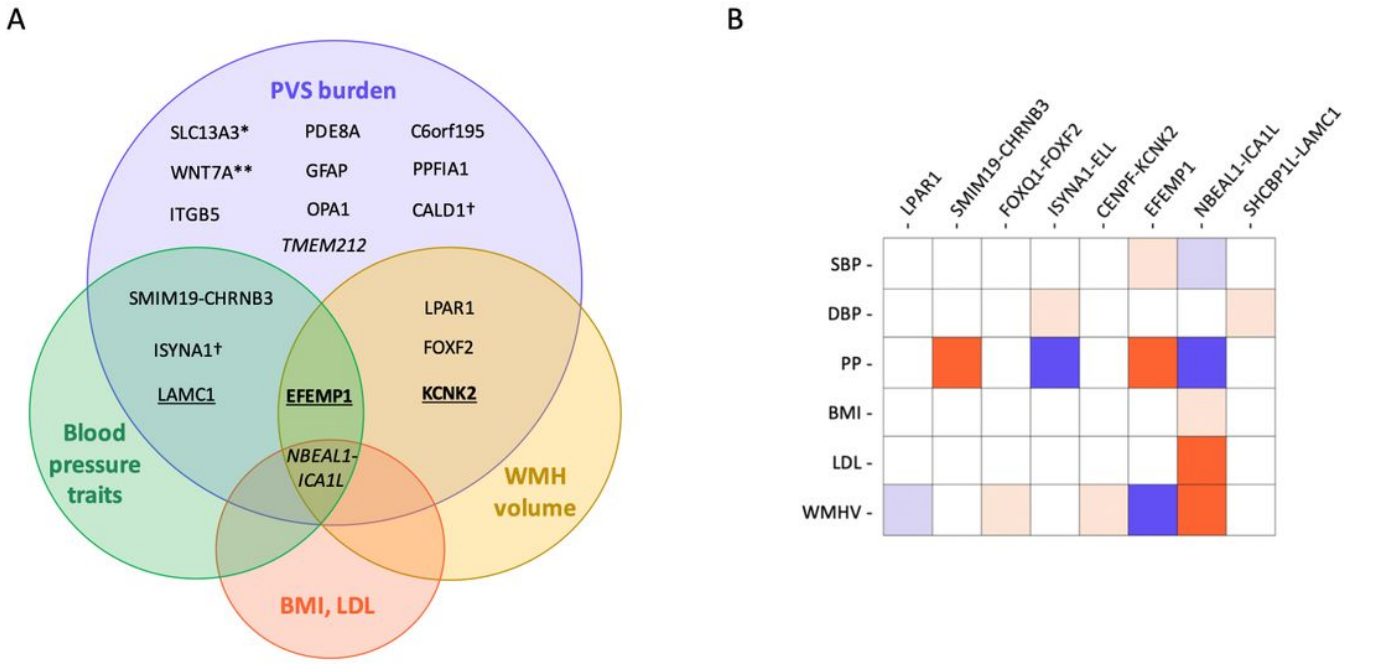

Figure 2

Association of PVS loci with vascular risk factors and other MRI-markers of SVD A. Venn diagram displaying significant association of genome-wide significant (GWS) risk loci for PVS with vascular risk factors and other MRI-markers of cSVD: in italic for BG PVS; underlined for HIP PVS (bold if also WGS for WM PVS); all others for WM PVS ($p<7.9x10-4$); * 6 independent loci; ** 2 independent loci; † genome-wide significant in Europeans only; B. Direction of association and level of significance of pleiotropic SNPs displayed in A: in red when the risk allele for extensive PVS burden is positively associated with the trait, in blue when the PVS risk allele is negatively associated with the trait (unexpected direction), in dark color for genome-wide significant associations, and in light color for significant association after multiple testing correction ($p<7.9x10-4$); PVS, perivascular spaces; SBP, systolic blood pressure; DBP, diastolic blood pressure; PP, pulse pressure; BMI, body mass index; LDL, LDL-cholesterol; WMH(V): white matter hyperintensity (volume).

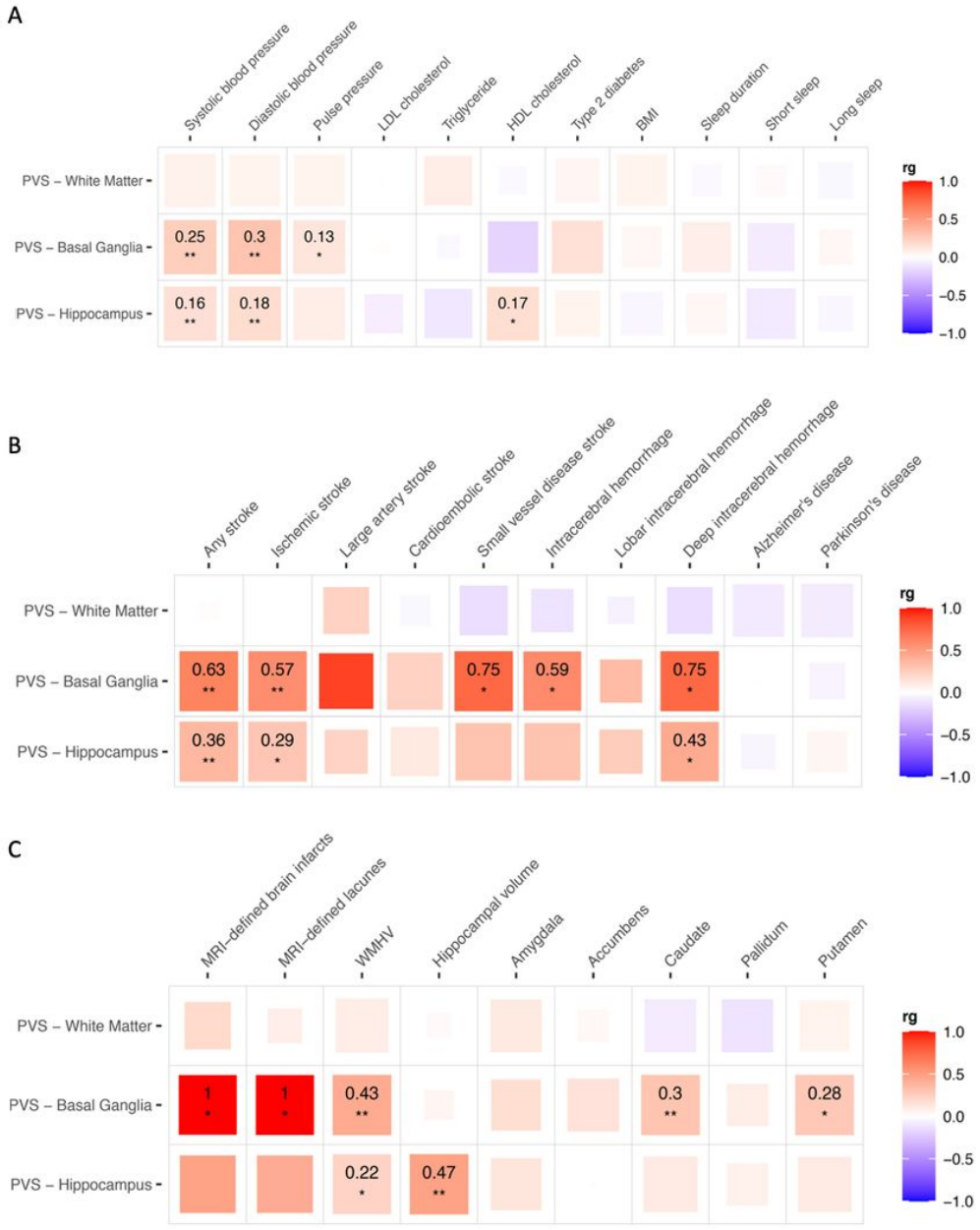

Figure 3

Genetic correlations of extensive PVS burden with risk factors, neurological diseases, and other MRI-markers of brain aging Genetic correlation using LDscore regression of extensive PVS burden with (A) putative risk factors, (B) neurological diseases, and (C) other MRI-markers of brain aging; LDSR: LD score regression; GSMR: Generalized Summary-data-based Mendelian Randomization; *p<0.05; **p<7.9x10-4 correcting for 21 independent phenotypes and the three PVS locations. Larger colored squares correspond to more significant p-values and the colors represent the direction of the genetic correlation (positive in red, negative in blue).

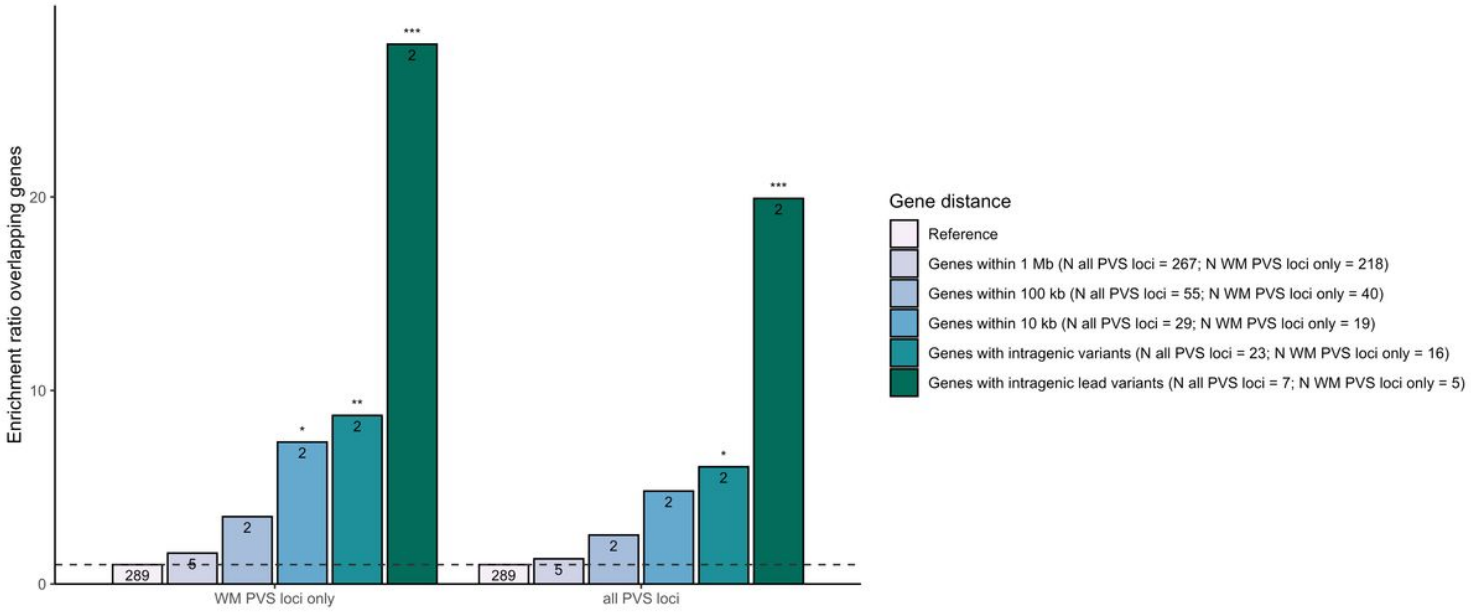

Figure 4

Enrichment of PVS risk loci in genes mutated in OMIM syndromes Enrichment of all PVS loci (left) and WM PVS loci only (right) in genes mutated in OMIM syndromes associated with WMH, leukodystrophy, leukoencephalopathy, stroke or dementia, according to distance from the lead variant; * p<0.05 ; ** p<(0.05/5); *** p<(0.05/5/2)

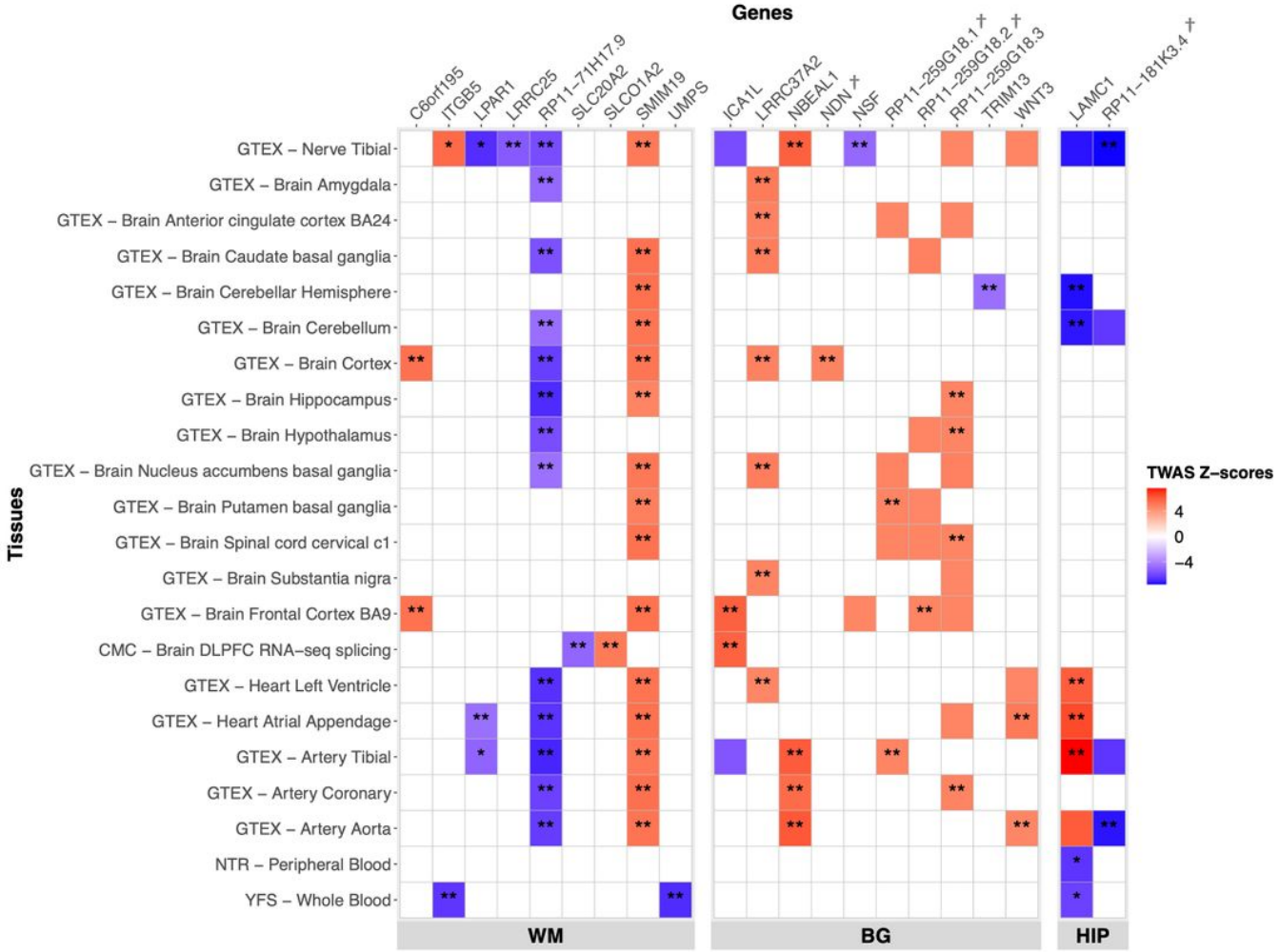

Figure 5

Transcriptome-wide significant genes with extensive PVS burden * significant result in the TWAS and conditional analyses; ** significant result in the TWAS and conditional analyses, and with a COLOC PP4 > 0.75; † genes in loci not identified in the GWAS

Supplementary Files

This is a list of supplementary files associated with this preprint. Click to download.

- PVSgenomicssupplementarytables021021subcorr.xlsx
- PVSgenomicssupplementaryappendix021021sub.docx
- flatDebetteepc.pdf
- flatDebetters.pdf